Alveolar macrophage–derived type I interferons orchestrate innate immunity to RSV through recruitment of antiviral monocytes

Michelle Goritzka,[1] Spyridon Makris,[1]* Fahima Kausar,[1]* Lydia R. Durant,[1] Catherine Pereira,[1] Yutaro Kumagai,[2] Fiona J. Culley,[1] Matthias Mack,[3] Shizuo Akira,[2] and Cecilia Johansson[1]

[1]Centre for Respiratory Infection, Respiratory Infections Section, National Heart and Lung Institute, Imperial College London, London W2 1PG, England, UK
[2]Laboratory of Host Defense, World Premier International Immunology Frontier Research Center, Osaka University, Suita, Osaka 565-0871, Japan
[3]University Hospital Regensburg, 93042 Regensburg, Germany

Type I interferons (IFNs) are important for host defense from viral infections, acting to restrict viral production in infected cells and to promote antiviral immune responses. However, the type I IFN system has also been associated with severe lung inflammatory disease in response to respiratory syncytial virus (RSV). Which cells produce type I IFNs upon RSV infection and how this directs immune responses to the virus, and potentially results in pathological inflammation, is unclear. Here, we show that alveolar macrophages (AMs) are the major source of type I IFNs upon RSV infection in mice. AMs detect RSV via mitochondrial antiviral signaling protein (MAVS)–coupled retinoic acid–inducible gene 1 (RIG-I)–like receptors (RLRs), and loss of MAVS greatly compromises innate immune restriction of RSV. This is largely attributable to loss of type I IFN–dependent induction of monocyte chemoattractants and subsequent reduced recruitment of inflammatory monocytes (infMo) to the lungs. Notably, the latter have potent antiviral activity and are essential to control infection and lessen disease severity. Thus, infMo recruitment constitutes an important and hitherto underappreciated, cell-extrinsic mechanism of type I IFN–mediated antiviral activity. Dysregulation of this system of host antiviral defense may underlie the development of RSV-induced severe lung inflammation.

CORRESPONDENCE
Cecilia Johansson:
c.johansson@imperial.ac.uk

Abbreviations used: AM, alveolar macrophage; BAL, bronchoalveolar lavage; FFU, focus-forming units; infMo, inflammatory monocyte; ISG, IFN-stimulated gene; MAVS, mitochondrial antiviral signaling protein; moDC, monocyte-derived DC; MOI, multiplicity of infection; pDC, plasmacytoid DC; p.i., postinfection; RIG-I, retinoic acid–inducible gene 1; RLR, RIG-I–like receptor; RSV, respiratory syncytial virus.

Respiratory syncytial virus (RSV) is an important human respiratory pathogen (Borchers et al., 2013). Infection with RSV manifests as a simple common cold in the majority of cases. However, in 2–3% of young children it leads to severe bronchiolitis and viral pneumonia, and it remains the major cause of infant hospitalization in the developed world. The variation in disease severity is caused by both host and viral factors and has previously been linked to polymorphisms in several innate immunity genes, including many that control the IFN system (Tal et al., 2004; Awomoyi et al., 2007; Janssen et al., 2007; Tulic et al., 2007; Siezen et al., 2009). IFNs may therefore be key regulators of RSV-induced lung inflammation, but it remains unclear which cell types and molecular pathways mediate IFN production in response to RSV infection and how IFNs then impact airway inflammation and bronchiolitis.

Type I IFNs, and the related group of type III IFNs, serve as a major innate immune barrier to viral infection. They can be produced rapidly by infected cells in response to viral invasion through engagement of cytosolic receptors that detect the presence of viral genomes or products of viral replication in the cytosol. In the case of RNA viruses such as RSV, the retinoic acid–inducible gene 1 (RIG-I)–like

*S. Makris and F. Kausar contributed equally to this paper.
Y. Kumagai's present address is Quantitative Immunology Research Unit, World Premier International Immunology Frontier Research Center, Osaka University, Suita, Osaka 565-0871, Japan.

The Rockefeller University Press $30.00
J. Exp. Med. 2015 Vol. 212 No. 5 699–714
www.jem.org/cgi/doi/10.1084/jem.20140825

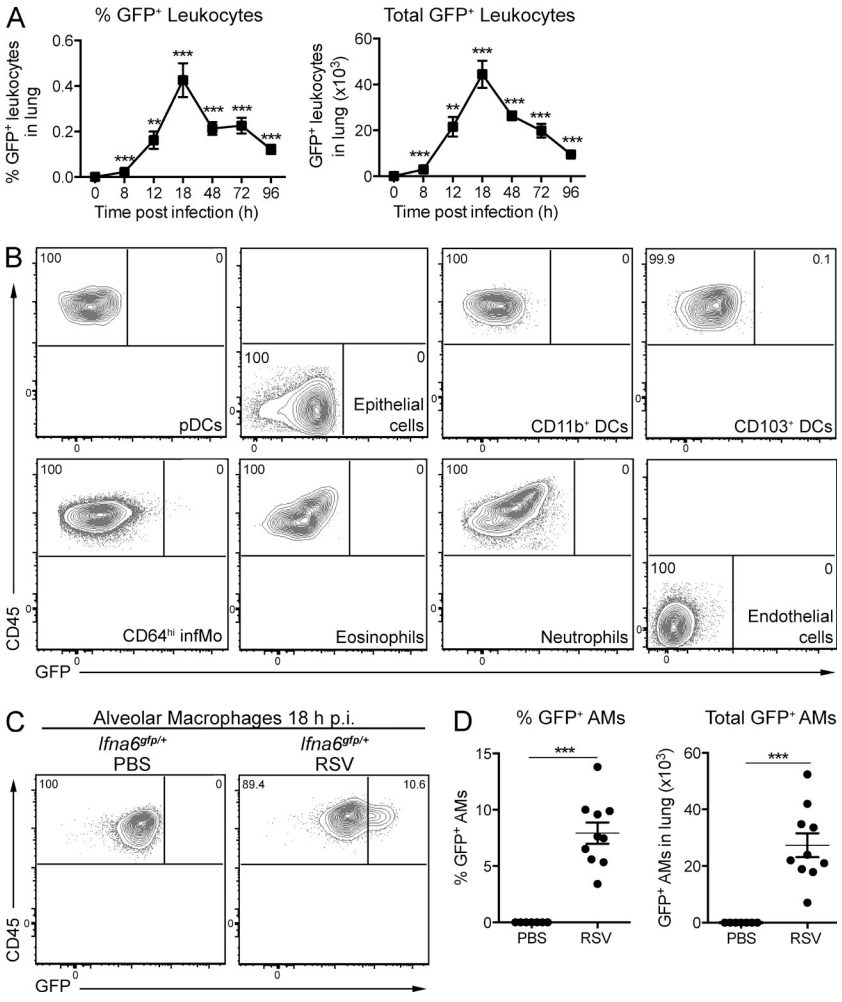

Figure 1. GFP+ AMs in RSV-infected *Ifna6*$^{gfp/+}$ mice. (A) Percentage and number of GFP+ pulmonary leukocytes in RSV-infected *Ifna6*$^{gfp/+}$ mice over time. 0 h represents mock (PBS)-infected mice. Data are mean ± SEM of five mice per group and representative of at least three independent experiments. (B) Representative flow cytometry plots of GFP expression in pDCs (CD11c^{int}CD11b^{lo}B220^{hi}Siglec-H^{hi}Ly6C^{hi}), epithelial cells (CD45^{lo}EpCAM^{hi}CD31^{lo}), CD11b+ DCs (CD11c^{hi}CD11b^{hi}CD64^{lo}Ly6C^{lo}), CD103+ DCs (CD11c^{hi}CD11b^{lo}CD103^{hi}), CD64+ inflammatory cells (CD11b^{hi}CD64^{hi}), eosinophils (CD11c^{lo}Siglec-F^{hi}), neutrophils (CD11b^{hi}Ly6G^{hi}), and endothelial cells (CD45^{lo}EpCAM^{lo}CD31^{hi}) from *Ifna6*$^{gfp/+}$ mice at 18 h p.i. (C) Representative plots of GFP expression in Siglec-F^{hi}CD11c^{hi} AMs from *Ifna6*$^{gfp/+}$ mice 18 h after mock (PBS) or RSV infection. In B and C, the data represent at least three independent experiments with five mice per experiment. (D) Percentage and total number of GFP+ AMs in the lungs 18 h after mock (PBS) or RSV infection. Each dot represents one mouse. Data are pooled from two independent experiments representing at least six experiments, and mean ± SEM of 10 mice is depicted. (A and D) Statistical significance of differences between mock (0 h)- and RSV-infected mice at different time points (A) and between mock (PBS)- and RSV-infected mice at 18 h p.i. (D) was determined by unpaired Student's *t* test. **, P < 0.01; ***, P < 0.001.

receptors (RLRs), RIG-I and melanoma differentiation–associated protein 5 (MDA5), sense atypical RNA species associated with viral infection (Liu et al., 2007; Loo et al., 2008; Yoboua et al., 2010; Goubau et al., 2013). Activated RLRs then signal through the adaptor, mitochondrial antiviral signaling protein (MAVS), to induce activation of transcription factors belonging to the nuclear NF-κB and IFN regulatory factor (IRF) families, which coordinately act to induce the transcription of type I and III IFN genes. Type I IFNs can also be produced via an RLR-independent manner by cells that detect the extracellular presence of virions or virus-infected cells. In such cases, members of the TLR family are often involved and RSV has been shown to trigger TLR2, TLR3, TLR4, and TLR7/8 (Marr et al., 2013).

Consistent with the fact that all cell types can be infected by viruses, every nucleated cell expresses RLRs and can produce type I IFNs via the cytosolic detection pathway. In contrast, the extracellular virus detection pathway via TLRs is predominantly active in immune cells, including macrophages and DCs, especially plasmacytoid DCs (pDCs). In the case of RSV, epithelial cells, fibroblasts, pDCs, alveolar macrophages (AMs), and conventional DCs have all been shown to produce type I IFNs after virus exposure in vitro (Jewell et al., 2007; Bhoj et al., 2008; Demoor et al., 2012; Schijf et al., 2013). Lung epithelial cells and pDCs have additionally been suggested to produce type I IFNs during experimental RSV infection in mice (Smit et al., 2006; Jewell et al., 2007). However, type I IFNs are notoriously difficult to detect in vivo as they are made only transiently. Thus, despite the genetic association between the type I IFN system and RSV disease, the cellular source of type I IFNs and the pathways leading to type I IFN production during RSV infection in vivo have not been truly elucidated.

Irrespective of source, all type I IFN species bind a single IFN-α/β receptor (IFNAR) expressed on all nucleated cells that signals through a JAK–STAT pathway to induce more than 300 IFN-stimulated genes (ISGs). These include components of the viral detection pathway themselves (e.g., RLRs), resulting in a positive feedback loop of virus-driven IFN production. ISGs also include a plethora of other genes whose products limit virus replication. For example, 2′-5′ oligoadenylate synthase 1 (OAS1), IFN-induced transmembrane protein 3 (IFITM3), or cyclic GMP-AMP synthase (cGAS) have all been shown to interfere with RSV replication

and limit productive infection (Behera et al., 2002; Everitt et al., 2013; Goubau et al., 2013; Schoggins et al., 2014). The cell-intrinsic control of viral replication by ISG products is thought to be a major component of the antiviral state conferred by type I IFN exposure and to underlie the ability of IFNs to protect healthy cells from viral infection (Goubau et al., 2013).

Our group recently found that, in addition to acting to limit viral infection, IFNAR signaling is also critical for inducing lung inflammation in response to RSV infection in mice (Goritzka et al., 2014). In the absence of IFNAR, proinflammatory cytokines and chemokines were not produced in RSV-infected lungs (Goritzka et al., 2014). This observation suggested that type I IFNs act in lung innate immunity beyond promoting cell-intrinsic viral control, by inducing inflammation. Type I IFN–driven lung inflammation could be a bystander phenomenon or a cell-extrinsic means of controlling virus infection through the recruitment of antiviral inflammatory cells. Here, we address which lung cell populations produce type I IFNs during RSV infection in vivo and how this translates into viral control. We show that the MAVS-dependent RLR pathway in AMs accounts for almost all type I IFN production in the lungs of RSV-infected mice. MAVS-dependent type I IFN production by AMs induces local production of monocyte chemoattractants and leads to the recruitment of inflammatory monocyte (infMo)–derived cells to the lung. Notably, the recruited cells have potent and nonredundant antiviral effects, which are essential to limit lung viral load and decrease disease severity. Our work indicates an underappreciated monocyte-dependent cell-extrinsic mechanism underlying the antiviral action of type I IFNs and highlights the importance of balanced lung inflammation in early antiviral defense. Dysregulation of type I IFN–mediated inflammation might offset its beneficial function and underlie the development of severe RSV disease.

RESULTS

Identification of pulmonary cell populations producing type I IFNs in response to RSV

Type I IFNs are produced transiently after viral infection, and the identification of IFN-producing cells in vivo can be problematic. To identify type I IFN–producing cells in the lungs of mice infected with RSV, we used *Ifna6*$^{gfp/+}$ mice, a transgenic model in which GFP is expressed under the control of the *Ifna6* promoter (Kumagai et al., 2007). Mice were i.n. infected with 2×10^6 focus-forming units (FFU) of RSV and followed over time. First, we monitored the level of GFP expression. GFP signal was first detectable at 8 h in CD45$^+$ leukocytes but not in CD45$^-$ cells (Fig. 1 A and not depicted). The percentage and number of GFP$^+$ leukocytes increased steadily from 8 to 18 h postinfection (p.i.) and declined thereafter (Fig. 1 A). Thus, *Ifna6*$^{gfp/+}$ mice appear to be a valid model for monitoring type I IFN expression in the lung after RSV challenge. The persistence of the GFP signal increases the likelihood of detecting relevant type I IFN–producing cells during the course of infection.

We assessed the presence of GFP signal in different lung cell types at 18 h p.i. by flow cytometry using the gating strategy shown in Fig. S1 (A and B). Although pDCs and epithelial cells are reported to be the main type I IFN producers during RSV infection (Smit et al., 2006; Jewell et al., 2007; Schijf et al., 2013), no GFP signal was detectable in either cell type (Fig. 1 B). Furthermore, there was no GFP expression in CD11b$^+$ DCs, CD103$^+$ DCs, CD64^{hi} inflammatory cells, eosinophils, neutrophils, or endothelial cells (Fig. 1 B). In contrast, around 7% of AMs displayed a detectable GFP signal (Fig. 1, C and D). Analysis at different time points confirmed the presence of GFP signal exclusively among AMs (Fig. 1, C and D; and not depicted). Of note, AMs up-regulated CD11b, a marker not normally expressed on that cell type, during the course of infection and GFP$^+$ AMs were all CD11b^{hi} after day 2 p.i. (not depicted).

To independently validate these findings and measure additional type I IFN species, CD45$^-$ and CD45$^+$ cells from naive or infected lungs from C57BL/6 mice were purified by cell sorting, and the levels of *Ifna5* and *Ifnb* mRNA were determined by quantitative RT-PCR (Fig. 2 A; for gating see Fig. S1 B). Concordant with the earlier results in Fig. 1, CD45$^-$ stromal cells expressed limited amounts of *Ifna5* and *Ifnb* when compared with CD45$^+$ cells (Fig. 2 A). To distinguish among the latter, different lung leukocyte cell populations were purified by cell sorting from infected *Ifna6*$^{gfp/+}$ mice (for gating strategy see Fig. S1, A and B). As expected, GFP$^+$ AMs contained the highest levels of *Ifna5* and *Ifnb* transcripts (Fig. 2 B). Low levels could also be detected in GFP$^-$ AMs and pDCs, arguing for slight underreporting in *Ifna6*$^{gfp/+}$ mice. In conclusion, AMs account for the majority of type I IFN production in the lungs of RSV-infected mice with only a minor contribution from pDCs.

Type I IFN production by AMs in response to RSV infection is RLR–MAVS dependent

Next we dissected the pathway leading to type I IFN induction by lung AMs. Live virus was necessary as UV-inactivated RSV administered i.n. did not elicit GFP expression (Fig. 3 A). Importantly, live virus failed to induce a GFP signal in AMs from *Ifna6*$^{gfp/+}$ mice deficient in the RLR adaptor protein MAVS (*Ifna6*$^{gfp/+}$ *Mavs*$^{-/-}$ mice; Fig. 3 A). This was true at all time points examined, from 8 to 96 h p.i. (Fig. 3 B), demonstrating a key role for the RLR pathway in the AM response to RSV. Consistent with that notion, primary AMs isolated from *Ifna6*$^{gfp/+}$ mice but not from *Ifna6*$^{gfp/+}$ *Mavs*$^{-/-}$ mice secreted large amounts of IFN-α in response to increasing doses of RSV ex vivo (Fig. 3 C). The lack of IFN-α production by *Ifna6*$^{gfp/+}$ *Mavs*$^{-/-}$ AMs was maintained even when the cells were stimulated with RSV up to multiplicities of infection (MOIs) of 20 (not depicted).

A previous study using Newcastle disease virus showed that loss of IFN-α production in *Mavs*$^{-/-}$ AMs leads to compensatory IFN-α secretion by pDCs (Kumagai et al., 2007). In contrast, no compensatory GFP$^+$ lung cell population was detectable at any time point (8 h to 9 d p.i.) in RSV-infected

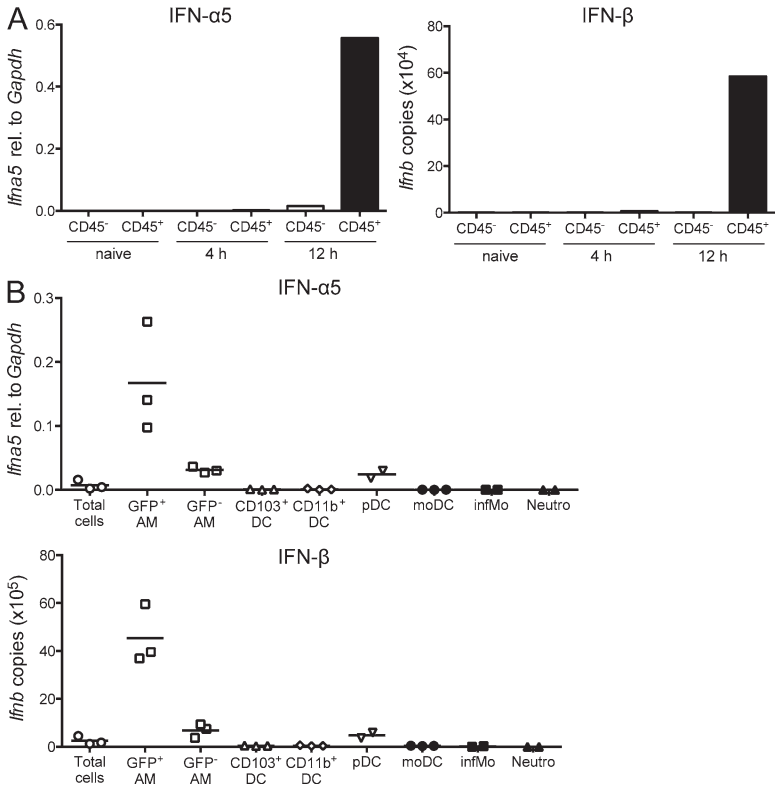

Figure 2. AMs are the main producers of type I IFNs in lungs of RSV-infected mice. (A) Lung cells from naive C57BL/6 mice or 4 and 12 h after RSV infection were sorted into CD45$^-$ and CD45$^+$ fractions. Expression of *Ifna5* and *Ifnb* mRNA was assessed by quantitative RT-PCR. One representative experiment of three is shown using pooled cells from five mice for each time point. (B) Lung leukocyte populations from *Ifna6*$^{gfp/+}$ mice at 18 h after RSV infection were sorted into GFP$^+$ and GFP$^-$ AMs (Siglec-F^{hi}CD11c^{hi}), CD103$^+$ DCs (CD11c^{hi}CD11b^{lo}CD103^{hi}), CD11b$^+$ DCs (CD11c^{hi}CD11b^{hi}CD64^{lo}Ly6C^{lo}), pDCs (CD11c^{int} CD11b^{lo}B220^{hi}Siglec-H^{hi}), moDCs (CD11b^{hi}CD64^{hi}CD11c^{hi}), infMos (CD11b^{hi}CD64^{hi}CD11c^{lo}), and neutrophils (CD11b^{hi} Ly6G^{hi}). Expression of *Ifna5* and *Ifnb* mRNA was assessed by quantitative RT-PCR. Each point depicts data from an individual experiment (two to three) with cells sorted from pools of 25–40 mice per experiment. The symbols represent different cell types as indicated, and the horizontal bars represent the mean.

Ifna6$^{gfp/+}$ *Mavs*$^{-/-}$ mice (not depicted). Furthermore, no expression of *Ifna5* or *Ifnb* was detected in sorted AMs, CD103$^+$ DCs, CD11b$^+$ DCs, or pDCs from *Ifna6*$^{gfp/+}$ *Mavs*$^{-/-}$ mice 18 h p.i. (not depicted). Consistent with the loss of GFP signal and the notion that AMs are the main producers of type I IFNs in this model, we found no type I IFNs (IFN-α3 and IFN-β) in total lung homogenates of infected *Ifna6*$^{gfp/+}$ *Mavs*$^{-/-}$ mice even though these cytokines were easily detected at 18 h p.i. in MAVS-sufficient *Ifna6*$^{gfp/+}$ controls (Fig. 3 D). Type III IFNs (IFN-λ2/3) or IFN-γ was also not detectable in the lungs of *Ifna6*$^{gfp/+}$ *Mavs*$^{-/-}$ mice (Fig. 3 E). Consistent with these results, induction of mRNAs encoding selected ISGs (Viperin, OAS-1, protein kinase R [PKR], or MX-1) was not observed in *Ifna6*$^{gfp/+}$ *Mavs*$^{-/-}$ mice but was detected shortly after infection in MAVS-sufficient *Ifna6*$^{gfp/+}$ controls (Fig. 3 F). Altogether, these data suggest that type I IFN–dependent antiviral responses to RSV are primarily caused by triggering of the RLR–MAVS pathway in AMs.

MAVS controls the innate immune response to RSV

To test whether loss of the type I IFN response to RSV affects the outcome of infection, we determined viral load in the lungs of *Ifna6*$^{gfp/+}$ (henceforth abbreviated WT) and *Ifna6*$^{gfp/+}$ *Mavs*$^{-/-}$ (henceforth abbreviated *Mavs*$^{-/-}$) mice. In accordance with previous studies by Bhoj et al. (2008) and Demoor et al. (2012), *Mavs*$^{-/-}$ mice had higher lung viral titers than control mice throughout the infection period and displayed delayed viral clearance (Fig. 4 A). Moreover, infection with RSV caused greater weight loss from day 6 until day 10 p.i. in *Mavs*$^{-/-}$ mice compared with MAVS-sufficient controls (Fig. 4 B). The bulk of the early inflammatory response to RSV infection was also strongly dependent on MAVS as transcripts encoding proinflammatory cytokines (e.g., TNF, IL-6, and IL-1β) were largely undetectable in lungs of *Mavs*$^{-/-}$ mice while being highly induced in control mice (Fig. 4 C; Bhoj et al., 2008). This is likely a secondary effect of the loss of type I IFNs as we have observed a similar phenotype in IFNAR1-deficient mice (Goritzka et al., 2014).

We further determined the effect of RSV infection on inflammatory cell recruitment to the lungs and extravasation into the airways. The recruitment of polymorphonuclear phagocytes, which occurs early after infection, was largely independent of MAVS as similar proportions and numbers of neutrophils were present in bronchoalveolar lavages (BALs; a representation of the airways) and lung cell suspensions from infected MAVS-sufficient and -deficient mice (Fig. 4, D and E). Consistent with this notion, substantial expression of the neutrophil chemoattractant *Cxcl1* was detected early after infection in both WT and *Mavs*$^{-/-}$ mice even though levels were higher in the former group (Fig. 4 F). Similarly, *Cxcl1* induction and unimpaired neutrophil recruitment was also observed in IFNAR1-deficient mice infected with RSV (Goritzka et al., 2014). The recruitment of T cells, including RSV-specific CD8$^+$ T cells, detected at day 8 p.i., also did not differ between WT and *Mavs*$^{-/-}$ mice (Fig. 4, G–I; Bhoj et al., 2008; Demoor et al., 2012). In contrast, we noticed a large difference between WT and *Mavs*$^{-/-}$ mice in lung accumulation of CD64^{hi} inflammatory cells after RSV infection.

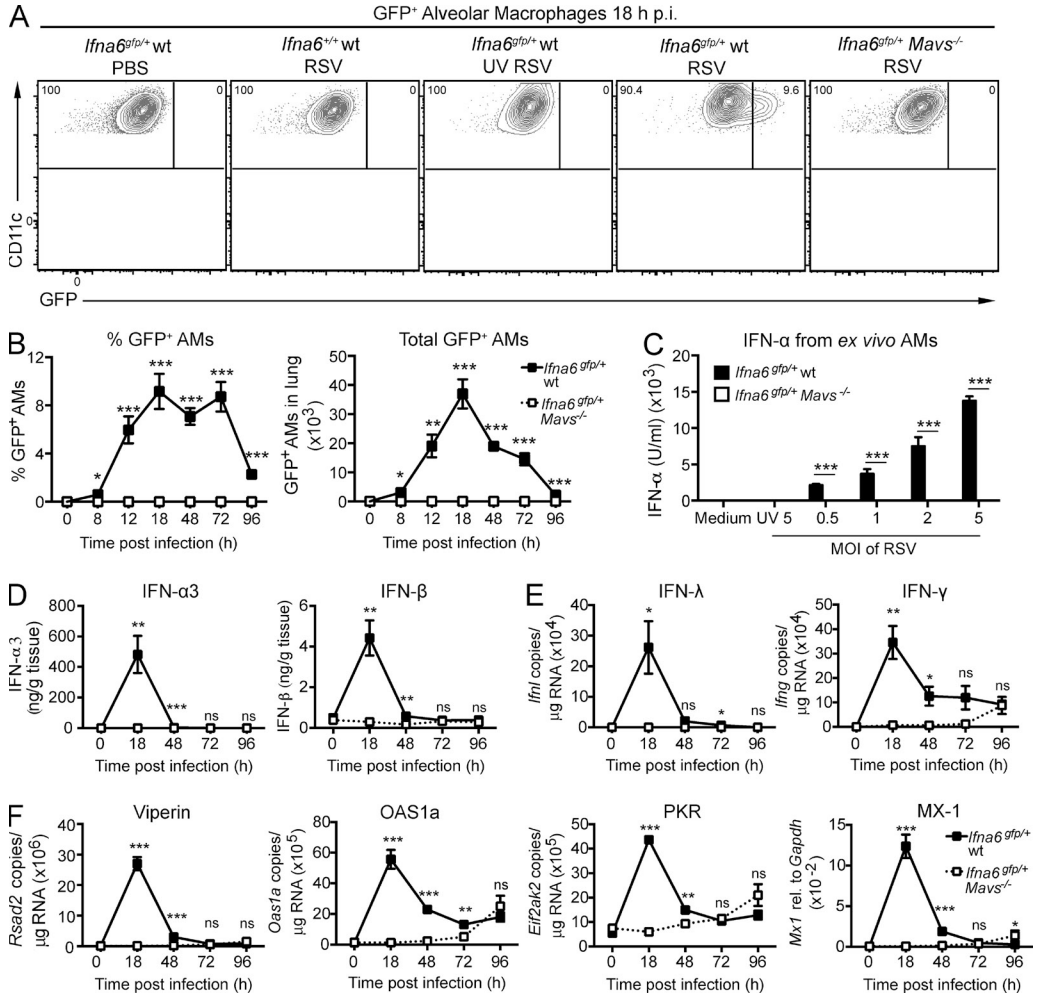

Figure 3. Type I IFN production by AMs is dependent on MAVS. (A) GFP expression in AMs from the indicated strains of mice was assessed 18 h after mock (PBS), RSV, or UV-inactivated RSV (UV RSV) instillation. (B) Percentage and number of GFP$^+$ AMs during the time course of RSV infection in *Ifna6*$^{gfp/+}$ and *Ifna6*$^{gfp/+}$ *Mavs*$^{-/-}$ mice. 0 h represents mock (PBS)-infected mice. (C) Secretion of IFN-α from primary AMs of the indicated genotypes after ex vivo exposure for 20 h to medium or the indicated MOIs of RSV or UV-RSV (MOI of 5; UV 5). (D) Analysis of IFN-α3 and IFN-β protein levels in lung homogenates from mice of the indicated genotypes at the indicated times p.i. (E and F) Levels of *Ifnl* and *Ifng* (E) and *Rsad2*, *Oas1a*, *Eif2ak2*, and *Mx1* transcripts (F) in lung tissue from mock (0 h)- or RSV-infected mice of the indicated genotypes at the indicated times p.i. Flow cytometry plots in A represent four to five mice per group and are representative of at least two independent experiments. Data in B and D–F are presented as mean ± SEM of four to five mice per group and are representative of at least two independent experiments. Statistical significance of differences between indicated genotypes at each time point was determined by unpaired Student's *t* test. Results in C are pooled from two independent experiments with at least three individual cultures per condition and presented as mean ± SEM. Statistical significance of differences between indicated groups was determined by unpaired Student's *t* test. *, $P < 0.05$; **, $P < 0.01$; ***, $P < 0.001$; ns, not significant.

In WT mice, leukocytes positive for CD64 and CD11b represented ∼40% of the total leukocyte population at day 2 p.i., but those cells were completely absent in lungs of *Mavs*$^{-/-}$ mice at all time points (Fig. 5, A and B). Thus, MAVS deficiency results in a general impairment of inflammatory cytokine production and absence of CD64^{hi} inflammatory cells in the lungs after RSV infection, but does not impact neutrophil or T cell recruitment.

infMos and monocyte-derived DCs (moDCs) are recruited to lungs of RSV-infected mice

Phenotypic characterization of the CD64^{hi} inflammatory cells recruited to the lungs of RSV-infected WT mice showed that most of these cells expressed Ly6C at day 1 p.i., suggestive of a monocytic origin. Ly6C expression was gradually down-regulated during the course of the infection (Fig. 5, C and D). Differential expression of CD11c further subdivided the CD64^{hi} inflammatory cells into what has previously been described as moDCs (CD11c^{hi}CD11b^{hi}CD64^{hi}) and infMos (CD11c^{lo}CD11b^{hi}CD64^{hi}; Fig. 5, C and E). The early recruited CD64^{hi} inflammatory cells were a mix of CD11c^{hi} moDCs and CD11c^{lo} infMos, whereas most of the cells by day 2 p.i. were CD11c^{hi} moDCs (Fig. 5 E). Interestingly, both moDCs and infMos produced TNF (Fig. 5, F and G; and not depicted; Shi and Pamer, 2011). Therefore, the lack of detectable TNF in the lungs of *Mavs*$^{-/-}$ mice infected

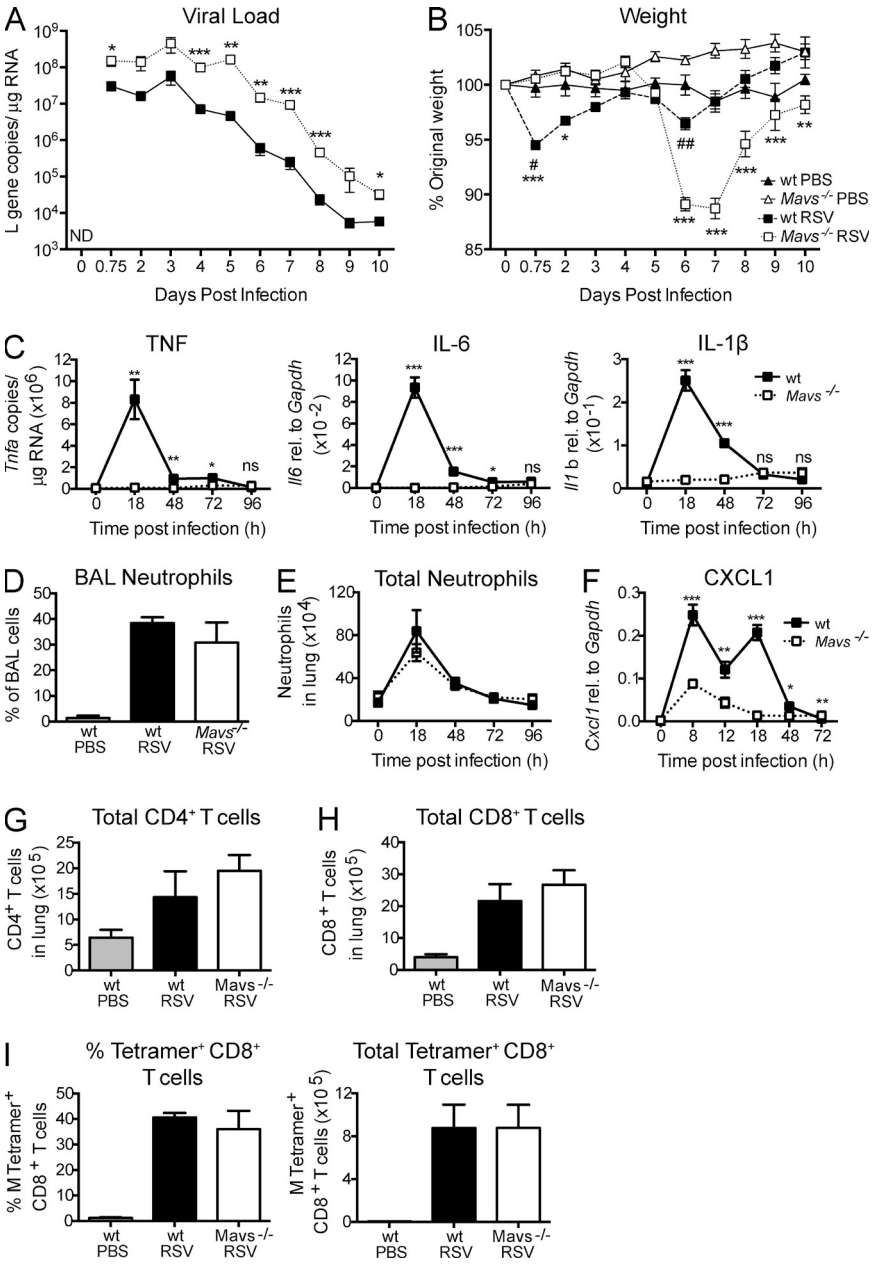

Figure 4. MAVS regulates innate resistance to RSV and modulates lung inflammation. (A and B) Lung viral load (A) and percentage of original weight (B) after RSV or mock (PBS) infection of the indicated strains was determined by quantification of viral L gene copies in lungs of RSV-infected mice and weighing at the indicated time points. Results are presented as mean ± SEM of 10 mice per group. (C) Levels of *Tnfa*, *Il6*, and *Il1b* transcripts in lung tissue from the indicated strains were measured by quantitative RT-PCR. 0 h represents mock (PBS)-infected mice. (D) BAL was obtained from mock- or RSV-infected WT or *Mavs*$^{-/-}$ mice on day 1 p.i. The frequency of neutrophils was determined using differential cell counting of H&E-stained cytospin slides. (E) Total number of lung neutrophils (CD11b^{+}Ly6G^{+}) was determined by flow cytometry (see gating in Fig. S1 A) in WT or *Mavs*$^{-/-}$ mice at different time points p.i. (F) Expression of *Cxcl1* in lung tissue from WT or *Mavs*$^{-/-}$ mice was measured by quantitative RT-PCR. (G and H) Number of CD4^{+} (G) and CD8^{+} (H) T cells in lung tissue from the indicated strains was quantified day 8 after RSV infection or after administration of PBS, as indicated. (I) RSV-specific CD8^{+} T cells were detected using $M_{187-195}$ tetramer staining on CD19^{-}, CD3^{+}, and CD8^{+} lung cells. Both frequency and total cell numbers are shown. In A and B, the data are pooled from two independent experiments. In C–I, the results are presented as mean ± SEM of five mice per group, and the data represent one of at least two independent experiments. In A and C–I, statistical significance of differences between WT or *Mavs*$^{-/-}$ mice at each time point was determined by unpaired Student's *t* test. In B, statistically significant differences between uninfected mice and infected WT mice are represented by "#" and between RSV-infected WT mice and *Mavs*$^{-/-}$ mice by "*." Statistical differences between groups were determined by two-way ANOVA with Bonferroni's post hoc test. #,*, $P < 0.05$; ##,**, $P < 0.01$; ***, $P < 0.001$; ns, not significant; ND, not detectable.

with RSV (Fig. 4 C) appears related to the failure to recruit CD64^{hi} inflammatory cells.

To confirm these conclusions, C57BL/6 mice were treated with an antibody against CCR2 (anti-CCR2), which depletes monocytes from the circulation and therefore prevents their migration into inflamed tissue (Mack et al., 2001). Confirming their monocytic origin, CD64^{hi} inflammatory cells were absent from the lungs of RSV-infected mice that had been treated with anti-CCR2 (Fig. 6, A and B). This was accompanied by a marked decrease in detectable TNF transcripts in the lungs (Fig. 6 C). Thus, CD64^{hi} inflammatory cells recruited to the lungs after RSV infection are derived from monocytes and are largely responsible for local TNF production.

AMs promote the recruitment of CD64^{hi} cells via type I IFN–dependent induction of monocyte chemoattractants

As *Mavs*$^{-/-}$ mice possess normal numbers of blood monocytes (not depicted), the failure of CD64^{hi} inflammatory cells to accumulate in lungs after infection was likely caused by a deficiency in recruitment. The chemoattractants CCL2, CCL7, and CCL12 (all ligands for CCR2) are critical for monocyte recruitment to inflamed tissues (Shi and Pamer, 2011). We found that all three chemokines were induced in lung tissue shortly after RSV infection in WT but not in *Mavs*$^{-/-}$ mice (Fig. 7, A and B). Type I IFNs have been implicated in the induction of CCL2 (Iijima et al., 2011; Majer et al., 2012; Conrady et al., 2013), and consistent with that notion, IFNAR1-deficient mice also failed to produce and

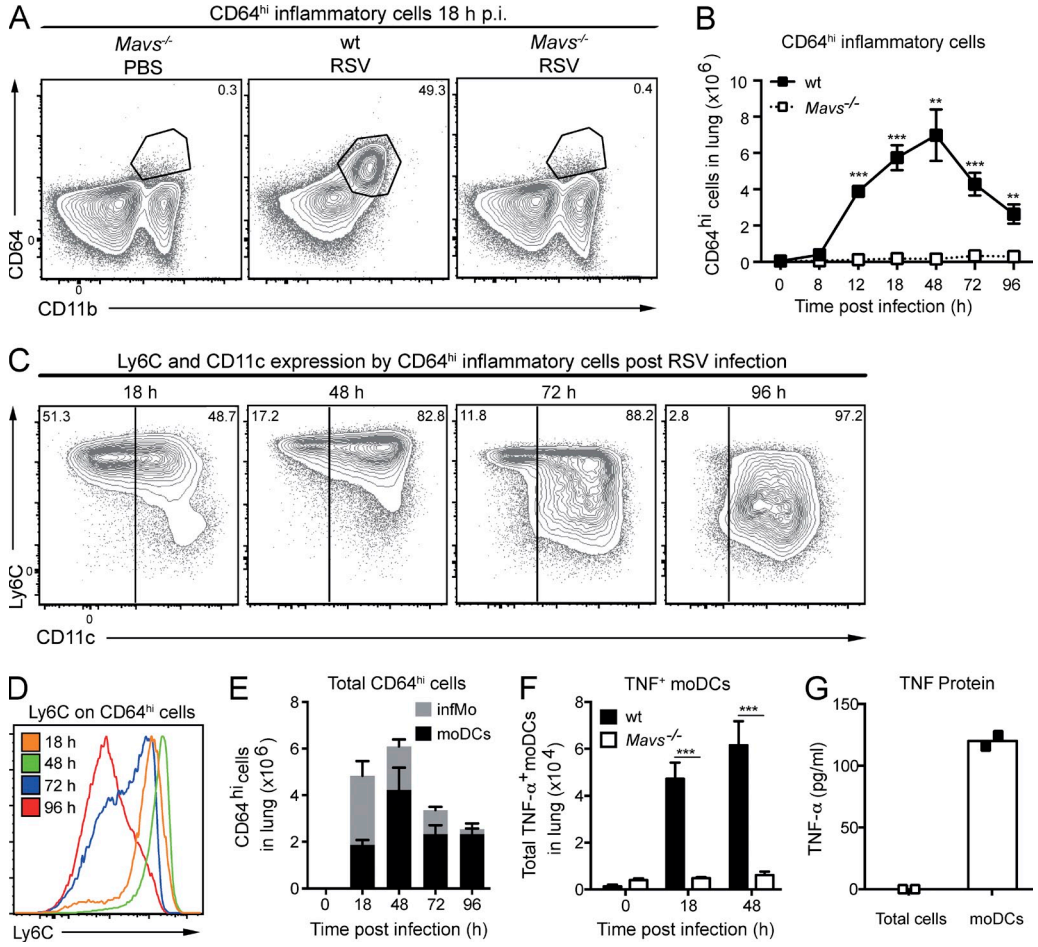

Figure 5. MAVS-dependent recruitment of TNF-producing CD64^{hi} inflammatory cells to RSV-infected lungs. (A) Representative plots of CD11b^{hi}CD64^{hi} inflammatory cells in the lungs of mock (PBS)- or RSV-infected WT or *Mavs*$^{-/-}$ mice 18 h p.i. with RSV. (B) Quantification of CD64^{hi} inflammatory cells in the lungs of WT and *Mavs*$^{-/-}$ mice during infection. Data are mean ± SEM of four to five mice per group. (C) Representative plots of Ly6C and CD11c expression on CD64^{hi}CD11b^{hi} inflammatory cells (gated as in Fig. S1 A) at the indicated time points after RSV infection of WT mice. (D) Representative histograms of Ly6C expression on CD64^{hi} inflammatory cells at the indicated time points p.i. of WT mice. (E) Quantification of the total number of CD64^{hi} cells split into CD11c^{hi} (moDCs; black) or CD11c^{lo} (infMos; gray) at the indicated time points p.i. of WT mice. Data are mean ± SEM of five mice per group. (F) Number of TNF-positive CD64^{hi}CD11c^{hi} moDCs in the lungs of WT or *Mavs*$^{-/-}$ mice at the indicated time points p.i. 0 h represents mock (PBS)-infected mice. Expression was determined by intracellular staining for TNF and flow cytometry analysis. Data are mean ± SEM of five mice per group. (G) Ex vivo production of TNF secreted into culture supernatants by total lung cells and FACS-sorted CD64^{hi}CD11c^{hi} moDCs isolated from WT mice at 18 h p.i. Each point represents one individual experiment using cells pooled from 25–40 mice. In A–F, the data are representative of at least two independent experiments. Statistical significance of differences between WT and *Mavs*$^{-/-}$ mice at different time points was determined by unpaired Student's *t* test. **, $P < 0.01$; ***, $P < 0.001$.

secrete CCL2 (Fig. 7 C) or recruit CD64^{hi} infMos to the lung after RSV infection (not depicted). We therefore hypothesized that the absence of CD64^{hi} inflammatory cell accumulation in the lungs of RSV-infected *Mavs*$^{-/-}$ mice and lack of local TNF production is caused by impaired monocyte recruitment through failure of AMs to produce type I IFNs and consequent lack of local induction of monocyte chemoattractants. To test this hypothesis, we first transferred WT AMs i.n. into *Mavs*$^{-/-}$ mice 24 h before RSV infection. This transfer led to an increase in CCL2 mRNA (48 h p.i.) in the lungs of *Mavs*$^{-/-}$ mice that had been reconstituted with WT AMs as compared with *Mavs*$^{-/-}$ mice that received *Mavs*$^{-/-}$ AMs (Fig. 7 D). Although the induction of CCL2 achieved with AM transfer did not reach the level observed in control-infected WT mice, it was nevertheless sufficient to partially restore accumulation of CD64^{hi} inflammatory cells (Fig. 7, E and F) and lead to increased expression of TNF (Fig. 7 G).

In a second approach, *Mavs*$^{-/-}$ mice were given a single administration of recombinant (r) IFN-α i.n. 6 h p.i. to mimic type I IFN secretion by AMs in WT mice. This was sufficient to induce expression of *Ccl2* (Fig. 8 A) and to partially restore recruitment of CD64^{hi} inflammatory cells (Fig. 8, B and C) and lung TNF levels (Fig. 8 D). Finally, in a third approach, we bypassed type I IFNs entirely and directly administered rCCL2 to the airways of *Mavs*$^{-/-}$ mice. After one dose of rCCL2 given 6 h p.i., CD64^{hi} inflammatory cells were attracted

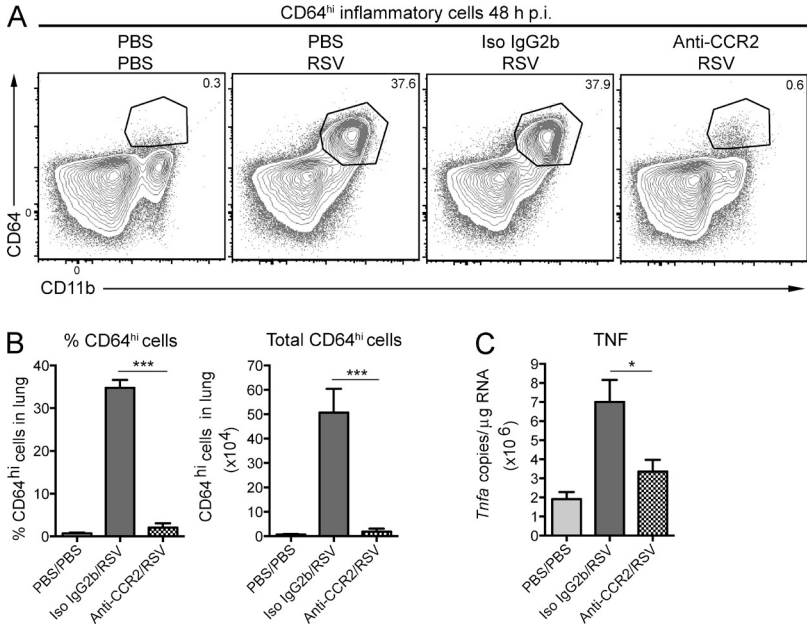

Figure 6. CD64^{hi} inflammatory cells are derived from monocytes and account for local TNF production. (A and B) Representative flow cytometry plots (A) and percentage and total number of CD11b^{hi}CD64^{hi} inflammatory cells in the lung (B) 48 h after RSV or mock (PBS) infection of C57BL/6 mice, pretreated with PBS, anti-CCR2, or IgG2b isotype–matched control antibody, as indicated. (C) *Tnfa* transcript levels in lung tissue from mice as in A and B determined by quantitative RT-PCR. In B and C, data are shown as mean ± SEM of 10 mice per group pooled from two independent experiments with 5 mice in each. Statistical significance of differences between the RSV-infected groups was determined by unpaired Student's *t* test. *, $P < 0.05$; ***, $P < 0.001$.

to the lungs (Fig. 8, E and F), and local production of TNF was restored (Fig. 8 G). NK cells were not recruited to lungs of the *Mavs*$^{-/-}$ mice with or without administration of rCCL2, acting as a control for specificity (Fig. 8 H). Together, these data indicate that AMs promote the recruitment of CD64^{hi} inflammatory cells to the lungs of RSV-infected mice through production of type I IFNs, which results in local induction of CCL2 and other monocyte chemoattractants and recruits CCR2^{+} monocytes.

CD64^{hi} inflammatory cells limit viral replication and disease severity

To address the role of the recruited CD64^{hi} inflammatory cells, we evaluated their contribution to disease severity, as measured by weight loss. As noted earlier, RSV-infected *Mavs*$^{-/-}$ mice showed greater weight loss than controls (Figs. 4 B and 9 A). Notably, this was completely prevented by prior transfer of WT but not *Mavs*$^{-/-}$ AMs (Fig. 9 A). Weight loss in mice correlates with increased viral load (Pribul et al., 2008). Indeed, RSV viral load was significantly lower in *Mavs*$^{-/-}$ mice that received WT AMs compared with *Mavs*$^{-/-}$ mice that were given *Mavs*$^{-/-}$ AMs (70–85% reduction of RSV N and L gene copies; Fig. 9 B). As the transfer of WT AMs into *Mavs*$^{-/-}$ mice results in type I IFN production, which can have pleiotropic and direct antiviral effects, we also used a depletion approach and found that viral load was increased in anti-CCR2–treated monocyte-depleted C57BL/6 mice despite normal production of type I IFNs (67–70% increase in RSV L and N gene copies; Fig. 9 C).

Finally, we administered rCCL2 to *Mavs*$^{-/-}$ mice to examine the ability of CD64^{hi} inflammatory cells to control disease in a setting that does not impact type I IFN induction. Remarkably, three doses of rCCL2 given during the course of infection almost completely prevented weight loss in *Mavs*$^{-/-}$ mice (Fig. 10 A). Viral load was also decreased as assessed by the measurement of L and N gene copies at days 2 (40–55% reduction in RSV N and L gene copies) and 4 p.i. (45–75% reduction in RSV N and L gene copies; Fig. 10 B). This is likely a large underestimate of the antiviral effect of CCL2 treatment because some of the antiviral effects of type I IFNs manifest themselves at points in the viral life cycle other than generation of viral RNA (such as, for example, viral packaging and budding [Goubau et al., 2013]). Indeed, when actual viral titers were measured (by an immunoplaque assay), lungs of *Mavs*$^{-/-}$ mice contained 100-fold higher virus levels at day 4 p.i. than controls, and this was nearly completely normalized by CCL2 treatment (Fig. 10 C). We conclude that the type I IFN–dependent influx of CD64^{hi} inflammatory cells into the lungs of RSV-infected mice is both necessary and sufficient to limit RSV replication and diminish disease severity. Indeed, it accounts for most of the resistance to RSV infection conferred by MAVS.

DISCUSSION

Type I IFNs can be produced by many cell types in response to virus encounter. They act through the IFNAR to induce a large number of genes encoding inhibitors of viral replication and virus assembly that together mediate cell-intrinsic resistance to virus infection and protect from viral spread. Genetic association studies have implicated a role for the type I IFN system in severe lung inflammation induced by RSV infection in some individuals. However, the cellular origin of those type I IFNs and the physiological role of type I IFN–induced inflammation remains unclear. Here, we show that AMs are responsible for production of type I IFNs during lower respiratory tract RSV infection and use the RLR–MAVS pathway for RSV detection. Notably, loss of type I IFN production by AMs results in increased viral

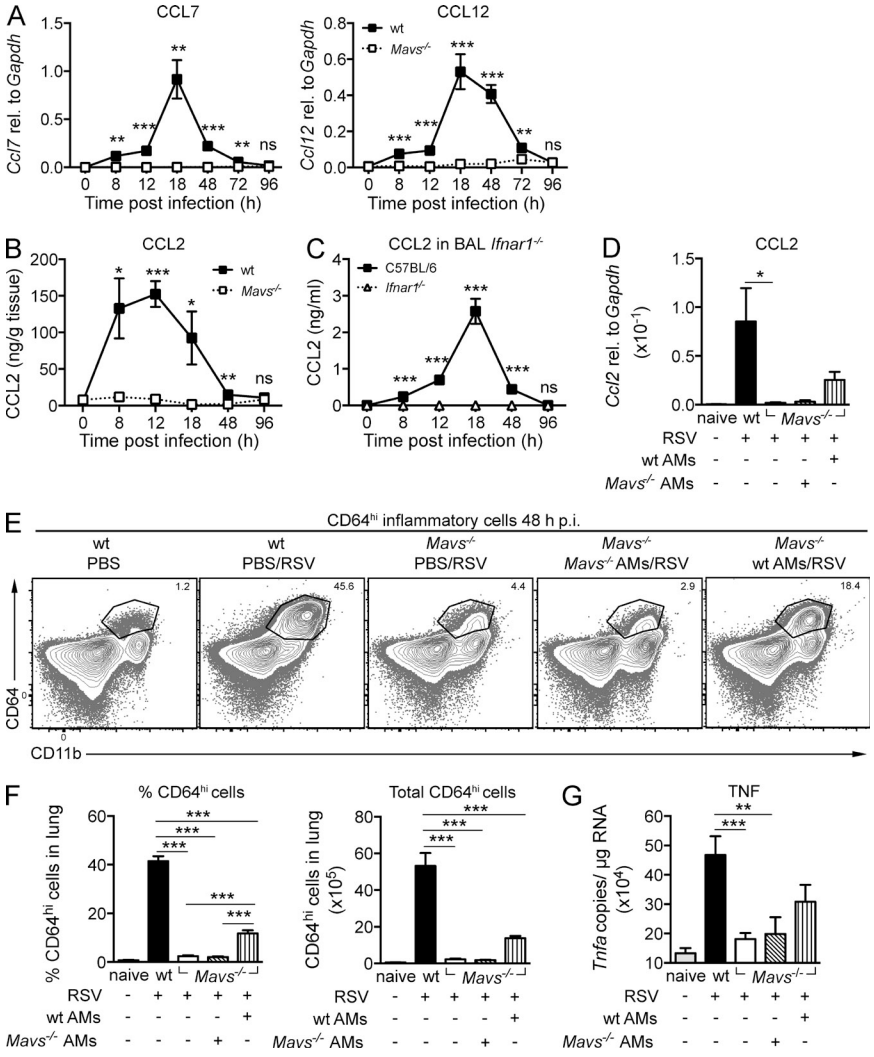

Figure 7. Transfer of WT AMs into *Mavs*$^{-/-}$ mice partially restores the recruitment of CD64^{hi} inflammatory cells upon RSV infection. (A) Expression of *Ccl7* and *Ccl12* in lung tissue of RSV- or mock (PBS)-infected (0 h) mice of the indicated strains as measured by quantitative RT-PCR. (B and C) Levels of CCL2 in lung homogenates from WT and *Mavs*$^{-/-}$ mice (B) and in BAL of C57BL/6 and *Ifnar1*$^{-/-}$ mice (C) were determined by ELISA. (D) Expression of *Ccl2* determined by quantitative RT-PCR in lung tissue of the indicated mouse strains 48 h after mock (PBS; stated as naive) or RSV infection. Mice received or not AMs of the indicated genotype i.n. 24 h before challenge. (E) Representative flow cytometry plots for CD11b^{hi}CD64^{hi} inflammatory cells in the lung 48 h after i.n. RSV or mock infection of WT, *Mavs*$^{-/-}$, or *Mavs*$^{-/-}$ mice given WT AMs or *Mavs*$^{-/-}$ AMs i.n. 24 h before infection as indicated. (F) Percentage and number of CD64^{hi} inflammatory cells in the lungs of mice treated as in D and E. (G) Expression of *Tnfa* determined by quantitative RT-PCR in the lungs of mice treated as in D and E. In A–C, data are mean ± SEM of four to five mice per group and are representative of two independent experiments. In D, F, and G, data are pooled from two independent experiments with 5 mice per group and are depicted as mean ± SEM of 10 mice. Statistical significance of differences between WT and *Mavs*$^{-/-}$ mice in A–C at each time point was determined by unpaired Student's *t* test. In D, F, and G, statistical differences between groups as indicated were determined by one-way ANOVA with Tukey's post hoc test. *, $P < 0.05$; **, $P < 0.01$; ***, $P < 0.001$; ns, not significant.

replication and exacerbated disease. However, this is not fully attributable to loss of cell-intrinsic viral control but, rather, is associated with lack of recruitment of monocyte-derived inflammatory cells. We further show that these inflammatory cells are both necessary and sufficient to mediate type I IFN–dependent control of RSV infection and to control RSV-induced pathology. Thus, our data reveal an underappreciated facet of type I IFN–dependent resistance to viral infection that operates in a cell-extrinsic fashion through rapid recruitment of antiviral infMos to sites of infection. They further suggest that type I IFN–dependent lung inflammation is a normal and important component of the antiviral response to RSV that, if dysregulated, might lead to severe disease in humans.

Most cells can produce type I IFNs, and epithelial cells, macrophages, fibroblasts, and pDCs have all been suggested as possible sources of these cytokines in response to RSV challenge (Jewell et al., 2007; Bhoj et al., 2008; Demoor et al., 2012). Most of those conclusions were based on studies involving in vitro exposure of cells to the virus, which may or may not reproduce virus accessibility in vivo. Using a mouse model of RSV infection, we found that the major source of type I IFN is in fact AMs. AMs have a crucial role in maintaining lung homeostasis and clearing airway debris (Hussell and Bell, 2014). Their strategic positioning at the air–liquid interface also places them at key sites of respiratory virus entry. Indeed, AMs have been shown to produce type I IFN after Newcastle disease virus and influenza A virus infection (Kumagai et al., 2007; Helft et al., 2012). Our data add to the notion that AMs are part of a rapid innate first line of defense against invading lung pathogens.

We found that the ability of AMs to rapidly respond to RSV depends on the adaptor protein MAVS, consistent with studies suggesting that RSV can be recognized through both RIG-I and MDA5 (Liu et al., 2007; Bhoj et al., 2008; Loo et al., 2008; Yoboua et al., 2010; Demoor et al., 2012). This also suggests that AMs are directly exposed to infectious virus in vivo as engagement of the RLR pathway requires viral RNA presence in the cytosol. Interestingly, RSV has been shown to infect AMs ex vivo, but infection does not result in production of infectious viral particles (Ravi et al., 2013). This suggests that AMs are naturally resistant to RSV replication,

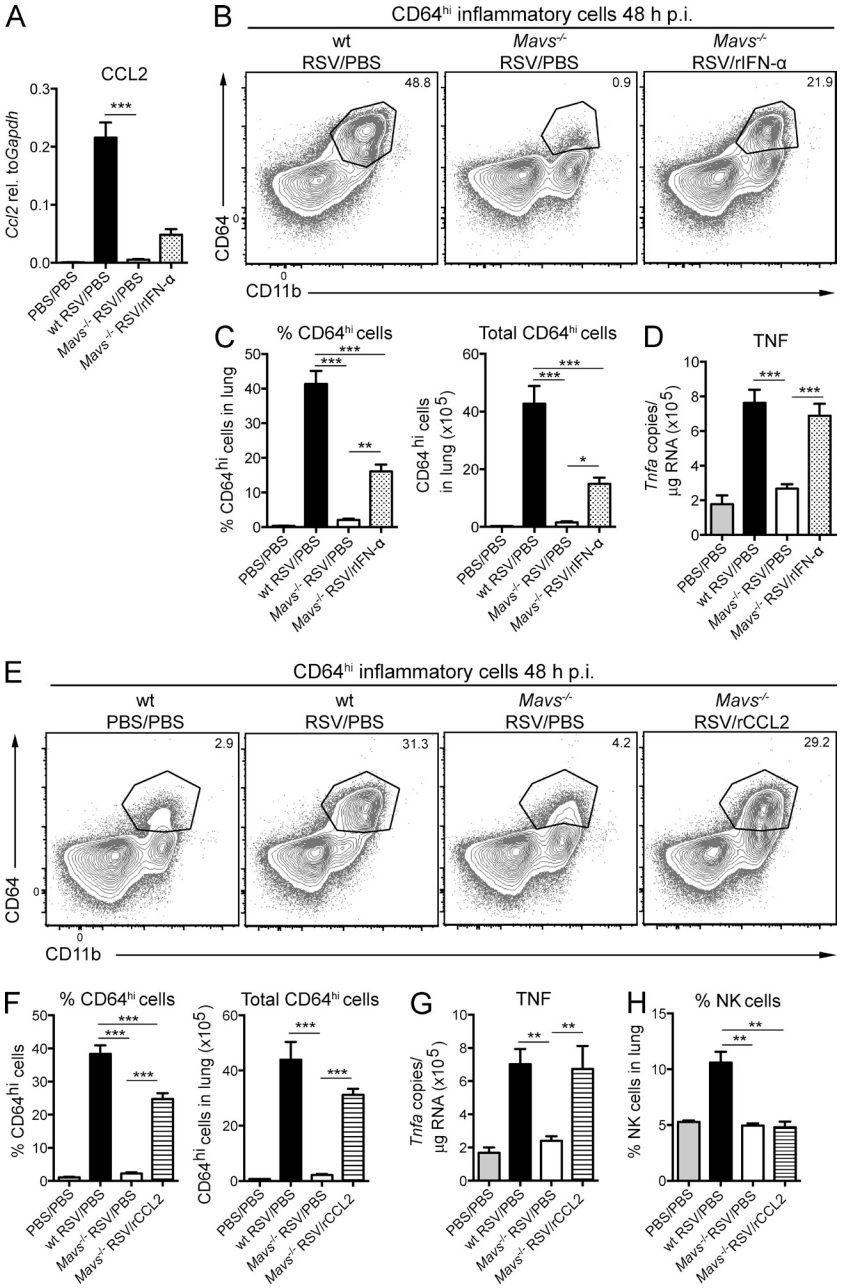

Figure 8. Recombinant IFN-α or CCL2 restores CD64^{hi} inflammatory cell recruitment in *Mavs*$^{-/-}$ mice after RSV infection. (A) Lung expression of *Ccl2* determined by quantitative RT-PCR 48 h after mock (PBS) or RSV infection of WT or *Mavs*$^{-/-}$ mice that received PBS or rIFN-α i.n. 6 h after RSV infection, as indicated. (B and C) Representative flow cytometry plots (B) and quantification of CD11b^{hi}CD64^{hi} inflammatory cells (C) in mice as in A. (D) Expression of *Tnfa* in mice as in A. (E) Representative flow cytometry plots of CD11b^{hi}CD64^{hi} inflammatory cells in the lung of mock (PBS)- or RSV-infected WT, *Mavs*$^{-/-}$, or *Mavs*$^{-/-}$ mice receiving PBS or rCCL2 at 6 h after RSV infection. Mice were analyzed 48 h p.i. (F) Quantification of CD64^{hi}CD11b^{hi} inflammatory cells in the lungs of mice as in E. (G) Expression of *Tnfa* in in the lungs of mice as in E. (H) Percentage of NK cells (CD3^{-}, NKp46^{+}) in lungs of the indicated groups of mice. In A, D, and H, data are mean ± SEM of five mice per group and are representative of two independent experiments. In C, F, and G, data are pooled from two independent experiments with 5 mice per group and are depicted as mean ± SEM of 10 mice. Statistical significance of differences between indicated groups was determined by one-way ANOVA with Tukey's post hoc test. *, P < 0.05; **, P < 0.01; ***, P < 0.001.

which may allow them to maintain sentinel activity while escaping the cytopathic effects of infection. Abortive viral replication may also render AMs less susceptible to the effect of the viral NS protein, which inhibits RLR activity (Spann et al., 2004; Ling et al., 2009; Boyapalle et al., 2012). NS protein–dependent blockade of the type I IFN responses could explain why lung epithelial cells do not register in our assays as a major source of type I IFN despite being the prevalent target of RSV infection and replication.

Local neutrophil and monocyte recruitment is a hallmark of inflammation. It occurs in response to chemokine production induced by inflammatory cytokines or by signals from receptors that detect infection or tissue injury. Consistent with that notion and previous data (Haeberle et al., 2001; Miller et al., 2004; Culley et al., 2006), we noticed that there is robust induction of CCL2, CCL7, and CCL12 in the lungs and recruitment of monocyte-derived cells early after RSV infection. This was not observed in *Mavs*$^{-/-}$ mice, but it was not a direct consequence of impaired RLR signaling in AMs. Rather, CCL2 production in several infection models is strongly dependent on type I IFN (Crane et al., 2009; Seo et al., 2011; Majer et al., 2012; Conrady et al., 2013), and we showed that the lack of type I IFN underlies the loss of CCL2. The cellular source of CCL2 during RSV infection in vivo is not known. A radioresistant cell type has been implicated in CCL2 production during HSV-1 infection of the cornea

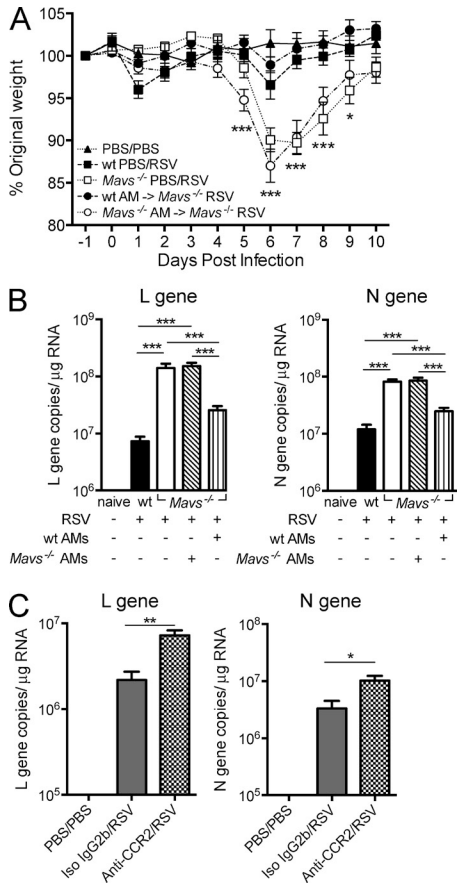

Figure 9. Availability of CD64^{hi} inflammatory cells correlates with outcome of RSV infection. (A) Percentage of original weight after RSV or mock (PBS) infection of the indicated strains, receiving or not WT AMs or *Mavs*$^{-/-}$ AMs 24 h before challenge (day 0). (B) Lung viral load in the indicated strains, receiving or not WT AMs or *Mavs*$^{-/-}$ AMs 24 h before RSV infection, was determined 48 h p.i. by quantitation of RSV L and N gene copies in lung tissue. Naive represents mock (PBS)-infected control mice. (C) Lung viral load in mock (PBS)- or RSV-infected C57BL/6 mice pretreated with isotype-matched control or anti-CCR2 antibody was determined 48 h p.i. by quantitation of RSV L and N gene copies in lung tissue. In A, data are mean ± SEM of five mice per group and are representative of two independent experiments. In B and C, data are pooled from two independent experiments with 5 mice per group and are depicted as mean ± SEM of 10 mice. In A, statistical significance of differences between *Mavs*$^{-/-}$ mice receiving WT AMs and *Mavs*$^{-/-}$ AMs was determined by two-way ANOVA with Bonferroni's post hoc test. In B and C, statistical significance between the indicated groups was determined by one-way ANOVA with Tukey's post hoc test in B and by unpaired Student's *t* test in C. *, $P < 0.05$; **, $P < 0.01$; ***, $P < 0.001$.

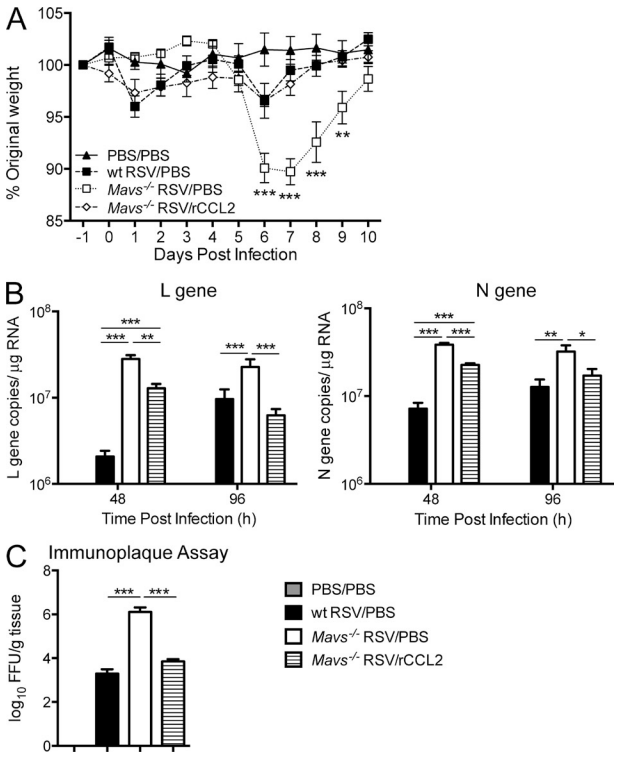

Figure 10. CD64^{hi} inflammatory cells are sufficient to control RSV infection. (A) Percentage of original weight in mock (PBS)- or RSV-infected WT or *Mavs*$^{-/-}$ mice with or without i.n. instillation of rCCL2 or PBS (as indicated) at 6, 18, and 48 h p.i. Day 0 indicates day of challenge. (B) Viral load in the indicated groups of mice (as in A) was determined by quantitation of RSV L and N gene copies in lung tissue at days 2 and 4 p.i. (C) Enumeration of infectious particles in lung tissue of the indicated groups of mice (see A) using an immunoplaque assay on day 4 p.i. Results in A–C are presented as mean ± SEM of five mice per group and are representative of two independent experiments. In A, statistical significance of differences between *Mavs*$^{-/-}$ mice receiving CCL2 and PBS was determined by two-way ANOVA with Bonferroni's post hoc test. Statistical significance between the indicated groups in B and C was determined by one-way ANOVA with Tukey's post hoc test. *, $P < 0.05$; **, $P < 0.01$; ***, $P < 0.001$.

(Conrady et al., 2013), and ex vivo infection using RSV elicited CCL2 production from both AMs and primary airway epithelial cells (Demoor et al., 2012). A possible source of CCL2 may be AMs themselves responding to their own type I IFN production through signaling via IFNAR, consistent with the notion that macrophages can be a source of monocyte chemoattractants (Deshmane et al., 2009).

The type I IFN–inducible monocyte chemoattractants mediate recruitment of monocyte-derived CD64^{hi} inflammatory cells, which make up as much as 40% of total lung leukocytes at day 2 after RSV infection and can be identified by high expression of CD11b and CD64. The latter has been argued to be a better marker than Ly6C for detection of monocyte progeny in the lung (Plantinga et al., 2013). Indeed, we found that Ly6C expression was down-regulated during the course of infection, especially from days 3 to 4 p.i. onwards. The CD64^{hi} inflammatory cells can be subdivided into CD11c^{lo} and CD11c^{hi} cells, representing infMos and moDCs, respectively (Shi and Pamer, 2011; Segura et al., 2013). Interestingly, CD11c expression on the CD64^{hi} inflammatory cells increased during infection, and almost all CD64^{hi} cells were positive for CD11c after day 2 of infection. CD11c upregulation has been interpreted as a sign of infMo conversion into moDCs, also known as Tip-DCs or inflammatory DCs

(Shi and Pamer, 2011; Segura et al., 2013). moDCs might play a role in local antigen acquisition, antigen presentation, and/or antigen transport to lymph nodes or restimulation of T cells in infected tissues, as suggested in other infection models (Serbina and Pamer, 2006; Iijima et al., 2011; Plantinga et al., 2013; Samstein et al., 2013). However, we did not detect impaired T cell responses in *Mavs*$^{-/-}$ mice compared with WT mice. Therefore, we focused on the function of recruited CD64^{hi} inflammatory cells in the early T cell–independent response to RSV. Interestingly, we observed that CD64^{hi} inflammatory cells play a major role in restricting virus production and dampening disease severity. Similarly, monocyte-derived cells have recently been shown to limit HSV-2 and HSV-1 replication in the vaginal tract and in the cornea, respectively (Iijima et al., 2011; Conrady et al., 2013).

The nature of the antiviral mechanism, whether it resides within the CD11c^{hi} or CD11c^{lo} population and how it limits disease severity remains unclear. It is possible that the antiviral activity is mediated in part by the production of TNF and/or inducible nitric oxide synthase (iNOS), consistent with the original function ascribed to Tip-DCs (Serbina et al., 2003). Increased RSV load has been observed in mice treated with anti-TNF (Rutigliano and Graham, 2004), and TNF can limit RSV replication in human lung epithelial cells (Merolla et al., 1995). Consistent with this notion, CD64^{hi} inflammatory cells in our model produced TNF and their absence led to a major loss of TNF in total lung extracts. Nitric oxide has also been implicated in monocyte-dependent antiviral control in a model of HSV-1 infection of the eye (Conrady et al., 2013). However, we failed to see an effect of iNOS inhibition on RSV lung titers in C57BL/6 mice (unpublished data) even though a study in BALB/c mice reported that it could increase infection (Stark et al., 2005). Another possibility could be that CD64^{hi} inflammatory cells express TNF-related apoptosis-inducing ligand (TRAIL) and kill RSV-infected epithelial cells, as reported for influenza virus infection (Herold et al., 2008; Davidson et al., 2014). However, we did not detect TRAIL expression on CD64^{hi} inflammatory cells during RSV infection (unpublished data). As for the impact of CD64^{hi} inflammatory cells on disease severity, it likely simply reflects their ability to control viral spread and thereby diminish the cytopathic effects of infection. However, CD64^{hi} inflammatory cells could also help promote epithelial cell repair via the secretion of trophic or antiinflammatory factors such as, for example, hepatocyte growth factor (Narasaraju et al., 2010) or prostaglandin E2 (Grainger et al., 2013). In this regard, it is interesting to note that CCL2 inhibition during influenza A virus infection can exacerbate epithelial damage (Narasaraju et al., 2010). We did not find prostaglandin production by CD64^{hi} inflammatory cells after RSV infection (unpublished data). Thus, the mechanism by which CD64^{hi} inflammatory cells mediate their antiviral effect and protect from disease remains elusive at present and is possibly multifactorial. Nevertheless, these cells are clearly a key component of resistance to the virus and constitute a cell-extrinsic mechanism of action of type I IFNs. Notably, the fact they are recruited and persist in the lung long after the production of type I IFNs has waned serves in part to temporally extend the antiviral effect of the cytokines and explains how the effects of the latter can manifest many days into the infection course.

IFNAR1- or MAVS-deficient mice infected with RSV ultimately recover and clear the virus, consistent with a key role for adaptive immune mechanisms in protection from the virus. Nevertheless, *Mavs*$^{-/-}$ mice lose more weight and display greater lung viral titers than control mice during RSV infection, implicating a cost in morbidity. Supporting this notion, viral titers in nasal washes from children with bronchiolitis have been shown to correlate positively with severity and duration of hospital stay (El Saleeby and Devincenzo, 2011; Scagnolari et al., 2012). We therefore propose that monocyte recruitment via the type I IFN–CCL2 axis is a natural component of the early inflammatory response to RSV infection, designed to keep the virus under control until lymphocyte-dependent protection takes over. However, monocyte-derived inflammatory cells can also induce tissue damage. For example, type I IFN– and CCL2-driven monocytosis induces lethal kidney pathology during experimental systemic infection with *Candida albicans* (Majer et al., 2012). Furthermore, infMos contribute to lung pathology in a model of influenza virus infection (Herold et al., 2008; Lin et al., 2008; Davidson et al., 2014), and CCL2 is increased in nasal secretions or BAL of children with RSV bronchiolitis (Garofalo et al., 2001; Welliver et al., 2002; McNamara et al., 2005). Lungs are particularly delicate, and unbridled inflammation at those sites can block gas exchange, with disastrous consequences for the host. Therefore, the production of type I IFNs and recruitment of antiviral monocytes during RSV infection must be carefully balanced to reduce viral load but not allow excessive cell infiltration. It is interesting to speculate that genetically or environmentally driven alterations to this balance possibly underlie the susceptibility of some human patients to RSV-induced bronchiolitis and pneumonia.

MATERIALS AND METHODS

Mice. C57BL/6 mice were purchased from Charles River or Harlan Laboratories, Inc. *Ifnar1*$^{-/-}$ mice on a C56BL/6 background were obtained from C. Reis e Sousa (London Research Institute, London, England, UK). *Ifna6*^{gfp} transgenic mice and *Ifna6*^{gfp} mice deficient in MAVS (*Mavs*$^{-/-}$; Kumagai et al., 2007) were used as heterozygotes (*Ifna6*$^{gfp/+}$). For all experiments in which GFP is not a primary readout (Fig. 4 onwards), the *Ifna6*$^{gfp/+}$ mice are designated as WT mice and *Ifna6*$^{gfp/+}$ *Mavs*$^{-/-}$ as *Mavs*$^{-/-}$ mice for simplicity and to denote the fact that the mice may or may not have a copy of the *gfp* insert at the *Ifna6* locus. In all experiments with genetically modified mice (e.g., *Mavs*$^{-/-}$ mice), littermates were always used as the control groups (e.g., WT mice). All mice were bred and maintained in pathogen-free conditions, and gender- and age-matched mice aged 7–12 wk were used for each experiment. All animal experiments were reviewed and approved by the Animal Welfare and Ethical Review Board (AWERB) within Imperial College London and approved by the UK Home Office in accordance with the Animals (Scientific Procedures) Act 1986 and the ARRIVE guidelines.

Virus and infections. Plaque-purified human RSV (originally A2 strain from the ATCC) was grown in HEp-2 cells (Lee et al., 2010). Inactivation was performed by exposing virus to UV light for 2 min in a CX-2000 UV

cross-linker (UVP). For infection, mice were lightly anesthetized and instilled i.n. with 1.5–2 × 10^6 FFU of RSV in 100 µl. In some instances, this was followed by i.n. instillation of recombinant proteins (500 ng/mouse IFN-α11 [Miltenyi Biotech] and 25 µg/mouse rCCL2 [PeproTech]) at 6 h p.i. For experiments monitoring the effect of CCL2 on weight loss and viral load day 4 p.i., rCCL2 (25 µg/mouse) was additionally given i.n. at 18 and 48 h p.i. For monocyte depletion, the anti-CCR2 antibody MC21 or an IgG2b isotype-matched control of irrelevant specificity (BD) was administered i.p. at 20 µg/mouse 6 h before and then daily during infection (Mack et al., 2001). For AM transfer into MAVS-deficient mice, 4–5 × 10^5 AMs pooled from 10 WT or *Mavs*$^{-/-}$ mice were administered via the i.n. route in 100 µl PBS 24 h before infection. RSV titer was assessed in fresh lungs 4 d after RSV infection using an immunoplaque assay (optimized from Loebbermann et al. [2012]). In brief, lung homogenate was titrated on HEp-2 cell monolayers in 96-well, flat-bottom plates and incubated for 2 h on a shaker. Then, pyruvate-free DMEM containing 2% FCS was added and the plate was further incubated for 20 h before being fixed with methanol and incubated with biotin-conjugated goat anti-RSV antibody (Biogenesis). Infected cells were detected using Streptavidin (Sigma-Aldrich) and DAB substrate (diaminobenzidine tetrahydrochloride), enumerated by light microscopy and used to calculate titer as FFU.

Isolation of lung cells. Mice were sacrificed at different times p.i. and perfused with PBS. To obtain lung leukocytes, lung lobes were collected into a C-Tube (Miltenyi Biotech) containing complete DMEM (cDMEM; supplemented with 10% fetal bovine serum, 2 mM L-glutamine, 100 U/ml penicillin, and 100 µg/ml streptomycin), 1 mg/ml Collagenase D (Roche) and 30 µg/ml DNase I (Invitrogen) and processed with a gentleMACS dissociator (Miltenyi Biotech) according to the manufacturer's protocol. Shredded tissue was incubated for 1 h at 37°C. After lysis of red blood cells, cells were strained through a 100-µm filter (BD). To obtain epithelial and endothelial cells, perfused lungs were injected and digested with 5 mg/ml Dispase (Roche) and 250 µg/ml DNase I (Sigma-Aldrich), as reported previously (Messier et al., 2012). Primary AMs for ex vivo stimulations and adoptive transfer were collected by BAL by flushing the lungs three times with 1 ml PBS supplemented with 5 mM EDTA (Life Technologies). The lavage was repeated twice, and AMs from several mice were pooled. The purity of AMs was >98% assessed by flow cytometry.

BAL cell processing. To determine the cellular composition of the BAL, cells were transferred onto a microscope slide (Thermo Fisher Scientific) using a Shandon Cytospin 3 centrifuge, and slides were stained with hematoxylin and eosin (H&E; Reagena, Gamidor). Cells were categorized as macrophages, lymphocytes, neutrophils, and eosinophils based on morphology and size under a light microscope (Axio; Carl Zeiss; Durant et al., 2014).

Flow cytometry. For staining, cells were first incubated for 30 min with fixable live-dead Aqua dye (Invitrogen), followed by incubation for 20 min with a purified rat IgG_{2b} anti–mouse CD16/CD32 receptor antibody (BD) to block Fc binding. Cells were then stained with fluorochrome-conjugated antibodies against CD11c (HL3, PE-CF594), CD11b (M1/70, AF700), CD45 (30-F11, eFluor780), Ly6C (HK1.4, eFluor450), CD103 (2E7, PerCP-Cy5.5), Siglec-H (eBio440c, eFluor660), B220 (RA3-6B2, eFluor450), Siglec-F (E50-2450, PE), CD64 (X54-5/7.1, APC), Ly6G (1A8, BV570), NKp46 (29A1.4, eFluor450), EpCAM (G8.8, PerCP-Cy5.5), and/or CD31 (MEC13.3, PE) in PBS containing 1% BSA, 5 mM EDTA, and 0.05% NaN_3 for 25 min at 4°C. The samples were analyzed without fixation on a standard BD LSRII equipped with 50-mW 405-nm, 50-mW 488-nm, 20-mW 633-nm lasers and an ND1.0 filter in front of the FSC photodiode. Acquisition was set to 500,000 live, single cells when pDC staining was included; otherwise, 250,000 live, single cells were acquired. For tetramer staining, cells were, after incubation with fixable live-dead Aqua dye (Invitrogen) and anti–mouse CD16/CD32 receptor antibody, stained with Alexa Fluor 647–conjugated $M_{187–195}$ tetramers (H-2D^b/NAITNAKII; obtained from the National Institutes of Health Tetramer Core Facility, Emory University, Atlanta, GA) for 30 min in the dark at room temperature. Surface staining was then performed using CD3 (145-2C11, PE-Cy7), CD4 (GK1.5, APC-H7), CD8 (53-6.7, AF700), and CD19 (1D3, FITC). Cells were fixed for 30 min in BD Cytofix/Cytoperm fixation buffer at 4°C, washed, and analyzed on a BD LSRFortessa equipped with 50-mW 405-nm, 50-mW 488-nm, 50-mW 561-nm, 20-mW 633-nm lasers and an ND1.0 filter in front of the FSC photodiode. Acquisition was set to 250,000 live, single cells. For intracellular staining for TNF, surface-stained and fixed cells (as described above) were stained with fluorochrome-conjugated anti-TNF (MP6-XT22, BV650) in the presence of purified rat IgG_{2b} anti–mouse CD16/CD32 receptor in BD permeabilization buffer for 60 min at 4°C. Samples were analyzed on a BD LSRFortessa-SORP equipped with 20-mW 355-nm, 50-mW 405-nm, 50-mW 488-nm, 50-mW 561-nm, 20-mW 633-nm lasers and an ND1.0 filter in front of the FSC photodiode. Acquisition was set to 250,000 live, single cells. All antibodies were purchased from BD, BioLegend, or eBioscience. Data were analyzed with FlowJo software (Tree Star).

FACS. For CD45$^{-/+}$ lung cell sorting, cells were, after dispase digestion of the lung tissue, stained as described above. For leukocyte cell sorting, lung single cell suspensions were incubated for 20 min with a purified rat IgG2b anti–mouse CD16/CD32 receptor antibody, after which CD11c enrichment was performed by incubating the lung cells with anti-CD11c microbeads (N418; Miltenyi Biotec) for 15 min on a shaker and positive selection on an autoMACS Pro Separator (Miltenyi Biotech). In some cases, the negative fraction was further processed to enrich for CD11c^{int} pDCs using anti-PDCA1 microbeads (Miltenyi Biotech). The positively selected cell fractions were stained as described above. Cells were then sorted using a standard BD Aria III equipped with 50-mW 405-nm, 50-mW 488-nm, 50-mW 561-nm, 20-mW 633-nm lasers and an ND1.5 filter in front of the FSC photodiode, a nozzle size of 100 µm, and corresponding BD FACSFlow sheath pressure of 20 psi, matched with a transducer frequency of 29 kHz. Input pressure was adjusted to ensure that every fifth to sixth drop was populated by an event. FACS-sorted cells were cultured overnight (see below) or stored in TRIzol until RNA extraction was performed.

RNA isolation and quantitative RT-PCR. Total RNA was isolated from homogenized lung tissue using an RNeasy Mini kit (QIAGEN) according to the manufacturer's instructions. RNA extraction from sorted cells was performed using TRIzol (Invitrogen) according to the manufacturer's instructions. After the chloroform step, the aqueous phase–containing RNA was further processed using the RNeasy Micro kit (QIAGEN) according to the manufacturer's instructions. 1 µg RNA (total lung) or 9 µl (FACS-sorted cells) was reverse transcribed using a High Capacity RNA-to-cDNA kit (Applied Biosystems) according to the manufacturer's instructions. To quantify mRNA levels in lung tissue, quantitative RT-PCR reactions for *Ifnl2/3*, *Ifnb*, *Tnfa*, *Ifng*, *Eif2ak2*, *Oas1a*, *Rsad2*, and RSV L and N gene were performed using primers and probes as previously described (Culley et al., 2002; Perkins et al., 2005; Lee et al., 2010; Slater et al., 2010; Bartlett et al., 2012; Goritzka et al., 2014). Analysis was performed using the QuantiTect Probe PCR Master Mix (QIAGEN) and the 7500 Fast Real-Time PCR System (Applied Biosystems). For absolute quantification, the exact number of copies of the gene of interest was calculated using a plasmid DNA standard curve, and the results were normalized to levels of *Gapdh*, a housekeeping gene (Applied Biosystems). For relative quantification, the expression of *Ifna5*, *Mx1*, *Ccl2*, *Cxcl1*, *Ccl7*, *Ccl12*, *Il6*, and *Il1b* (all from Applied Biosystems) was expressed relatively to the expression of *Gapdh*. First, the ΔCt (Ct = cycle threshold) between the target gene and *Gapdh* for each sample was calculated, after the calculation of $2^{-\Delta Ct}$. Analysis was performed using 7500 Fast System SDS Software (Applied Biosystems).

Chemokine and cytokine detection. Lungs were placed in protease inhibitor cocktail (Roche) on ice and homogenized using a TissueLyser (QIAGEN). Homogenate was centrifuged for 10 min, 10,000 *g* at 4°C, and chemokine and cytokine quantification was then performed on the supernatant.

For chemokine and cytokine quantification in the airways, BAL fluid was collected by flushing the lungs three times with 1 ml PBS supplemented with 5 mM EDTA (Life Technologies). For ex vivo AM stimulation, 1.25×10^5 AMs/well were seeded into 96-well plates. After 2 h at 37°C, cells were washed and exposed to different MOIs of RSV. After 20 h, supernatants were collected for cytokine analysis. The concentration of CCL2 was measured using mouse DuoSet ELISA (R&D Systems) according to the manufacturer's instructions. IL-6 was detected by ELISA using MP5-20F3 capture antibody and biotinylated MP5-32C11 detection antibody (both from BD). IFN-α was detected by ELISA as previously described (Asselin-Paturel et al., 2001). Data were acquired on a SpectraMax Plus plate reader (Molecular Devices) and analyzed using SoftMax software (version 5.2). IFN-α3 and IFN-β levels were determined using a Procarta Immunoassay (Affymetrix). Data were acquired with a Bio-Plex 200 system (Bio-Rad Laboratories). The concentration of cytokines in each sample was determined by reference to a standard curve using the Bio-Plex 6 software (Bio-Rad Laboratories). For ex vivo production of TNF by moDCs, FACS-sorted moDCs or total lung cells from 18 h p.i. were seeded at 10^5 cells/well in cDMEM. After 18-h incubation at 37°C, supernatants were assessed for TNF presence by Luminex (20-Plex Luminex kit; Life Technologies).

Statistical analysis. Statistical analysis was performed using Prism 6 (GraphPad Software). Two group comparisons were performed using unpaired, two-tailed Student's *t* test. One-way ANOVA with Tukey's post hoc test was used to compare multiple groups, and two-way ANOVA with Bonferroni's post hoc test was used for time-kinetic comparison of weight loss. Data are expressed as the mean ± SEM, and for all tests a value of $P < 0.05$ was considered as significant. *, $P < 0.05$; **, $P < 0.01$; ***, $P < 0.001$; ns, not significant.

Online supplemental material. Fig. S1 shows gating strategy for identifying and sorting lung cell populations using flow cytometry. Online supplemental material is available at http://www.jem.org/cgi/content/full/jem.20140825/DC1.

We thank Peter Openshaw for advice and continuous support. We also thank Caetano Reis e Sousa and Malte Paulsen for critically reading the manuscript. We thank the National Institutes of Health Tetramer Core Facility for RSV $M_{187-195}$ tetramers (H-2D^b/NAITNAKII) and staff of the St. Mary's Flow Cytometry Facility and the Animal Facility for their assistance.

C. Johansson is supported by a Career Development Award from the Medical Research Council (grant G0800311) and by a research grant from the Rosetrees Trust (M370). M. Goritzka, S. Makris, and F. Kausar are supported by PhD Fellowships from the National Heart and Lung Institute Foundation (registered charity number 1048073).

The authors declare no competing financial interests.

Author contributions: M. Goritzka designed, performed, and analyzed the experiments and wrote the paper. S. Makris, F. Kausar, L.R. Durant, and C. Pereira performed specific experiments and reviewed the paper. F.J. Culley provided advice and reviewed the manuscript. Y. Kumagai and S. Akira generated and provided *Ifna6*^{gfp} mice. M. Mack provided anti-CCR2 antibody and advice for depletion on CCR2$^+$ monocytes. C. Johansson supervised the project, designed the experiments, and wrote the paper.

Submitted: 30 April 2014
Accepted: 24 March 2015

REFERENCES

Asselin-Paturel, C., A. Boonstra, M. Dalod, I. Durand, N. Yessaad, C. Dezutter-Dambuyant, A. Vicari, A. O'Garra, C. Biron, F. Brière, and G. Trinchieri. 2001. Mouse type I IFN-producing cells are immature APCs with plasmacytoid morphology. *Nat. Immunol.* 2:1144–1150. http://dx.doi.org/10.1038/ni736

Awomoyi, A.A., P. Rallabhandi, T.I. Pollin, E. Lorenz, M.B. Sztein, M.S. Boukhvalova, V.G. Hemming, J.C.G. Blanco, and S.N. Vogel. 2007. Association of TLR4 polymorphisms with symptomatic respiratory syncytial virus infection in high-risk infants and young children. *J. Immunol.* 179:3171–3177. http://dx.doi.org/10.4049/jimmunol.179.5.3171

Bartlett, N.W., L. Slater, N. Glanville, J.J. Haas, G. Caramori, P. Casolari, D.L. Clarke, S.D. Message, J. Aniscenko, T. Kebadze, et al. 2012. Defining critical roles for NF-κB p65 and type I interferon in innate immunity to rhinovirus. *EMBO Mol. Med.* 4:1244–1260. http://dx.doi.org/10.1002/emmm.201201650

Behera, A.K., M. Kumar, R.F. Lockey, and S.S. Mohapatra. 2002. 2′-5′ Oligoadenylate synthetase plays a critical role in interferon-γ inhibition of respiratory syncytial virus infection of human epithelial cells. *J. Biol. Chem.* 277:25601–25608. http://dx.doi.org/10.1074/jbc.M200211200

Bhoj, V.G., Q. Sun, E.J. Bhoj, C. Somers, X. Chen, J.P. Torres, A. Mejias, A.M. Gomez, H. Jafri, O. Ramilo, and Z.J. Chen. 2008. MAVS and MyD88 are essential for innate immunity but not cytotoxic T lymphocyte response against respiratory syncytial virus. *Proc. Natl. Acad. Sci. USA.* 105:14046–14051. http://dx.doi.org/10.1073/pnas.0804717105

Borchers, A.T., C. Chang, M.E. Gershwin, and L.J. Gershwin. 2013. Respiratory syncytial virus—a comprehensive review. *Clin. Rev. Allergy Immunol.* 45:331–379. http://dx.doi.org/10.1007/s12016-013-8368-9

Boyapalle, S., T. Wong, J. Garay, M. Teng, H. San Juan-Vergara, S. Mohapatra, and S. Mohapatra. 2012. Respiratory syncytial virus NS1 protein colocalizes with mitochondrial antiviral signaling protein MAVS following infection. *PLoS ONE.* 7:e29386. http://dx.doi.org/10.1371/journal.pone.0029386

Conrady, C.D., M. Zheng, N.A. Mandal, N. van Rooijen, and D.J.J. Carr. 2013. IFN-α-driven CCL2 production recruits inflammatory monocytes to infection site in mice. *Mucosal Immunol.* 6:45–55. http://dx.doi.org/10.1038/mi.2012.46

Crane, M.J., K.L. Hokeness-Antonelli, and T.P. Salazar-Mather. 2009. Regulation of inflammatory monocyte/macrophage recruitment from the bone marrow during murine cytomegalovirus infection: role for type I interferons in localized induction of CCR2 ligands. *J. Immunol.* 183:2810–2817. http://dx.doi.org/10.4049/jimmunol.0900205

Culley, F.J., J. Pollott, and P.J.M. Openshaw. 2002. Age at first viral infection determines the pattern of T cell–mediated disease during reinfection in adulthood. *J. Exp. Med.* 196:1381–1386. http://dx.doi.org/10.1084/jem.20020943

Culley, F.J., A.M.J. Pennycook, J.S. Tregoning, T. Hussell, and P.J.M. Openshaw. 2006. Differential chemokine expression following respiratory virus infection reflects Th1- or Th2-biased immunopathology. *J. Virol.* 80:4521–4527. http://dx.doi.org/10.1128/JVI.80.9.4521-4527.2006

Davidson, S., S. Crotta, T.M. McCabe, and A. Wack. 2014. Pathogenic potential of interferon αβ in acute influenza infection. *Nat. Commun.* 5:3864. http://dx.doi.org/10.1038/ncomms4864

Demoor, T., B.C. Petersen, S. Morris, S. Mukherjee, C. Ptaschinski, D.E. De Almeida Nagata, T. Kawai, T. Ito, S. Akira, S.L. Kunkel, et al. 2012. IPS-1 signaling has a nonredundant role in mediating antiviral responses and the clearance of respiratory syncytial virus. *J. Immunol.* 189:5942–5953. http://dx.doi.org/10.4049/jimmunol.1201763

Deshmane, S.L., S. Kremlev, S. Amini, and B.E. Sawaya. 2009. Monocyte chemoattractant protein-1 (MCP-1): an overview. *J. Interferon Cytokine Res.* 29:313–326. http://dx.doi.org/10.1089/jir.2008.0027

Durant, L.R., C. Pereira, A. Boakye, S. Makris, F. Kausar, M. Goritzka, and C. Johansson. 2014. DNGR-1 is dispensable for CD8$^+$ T-cell priming during respiratory syncytial virus infection. *Eur. J. Immunol.* 44:2340–2348. http://dx.doi.org/10.1002/eji.201444454

El Saleeby, C.M., and J.P. Devincenzo. 2011. Respiratory syncytial virus load and disease severity in the community. *J. Med. Virol.* 83:904–905. http://dx.doi.org/10.1002/jmv.22039

Everitt, A.R., S. Clare, J.U. McDonald, L. Kane, K. Harcourt, M. Ahras, A. Lall, C. Hale, A. Rodgers, D.B. Young, et al. 2013. Defining the range of pathogens susceptible to Ifitm3 restriction using a knockout mouse model. *PLoS ONE.* 8:e80723. http://dx.doi.org/10.1371/journal.pone.0080723

Garofalo, R.P., J. Patti, K.A. Hintz, V. Hill, P.L. Ogra, and R.C. Welliver. 2001. Macrophage inflammatory protein-1alpha (not T helper type 2 cytokines) is associated with severe forms of respiratory syncytial virus bronchiolitis. *J. Infect. Dis.* 184:393–399. http://dx.doi.org/10.1086/322788

Goritzka, M., L.R. Durant, C. Pereira, S. Salek-Ardakani, P.J.M. Openshaw, and C. Johansson. 2014. Alpha/beta interferon receptor signaling amplifies early proinflammatory cytokine production in the lung during

respiratory syncytial virus infection. *J. Virol.* 88:6128–6136. http://dx.doi.org/10.1128/JVI.00333-14

Goubau, D., S. Deddouche, and C. Reis e Sousa. 2013. Cytosolic sensing of viruses. *Immunity*. 38:855–869. http://dx.doi.org/10.1016/j.immuni.2013.05.007

Grainger, J.R., E.A. Wohlfert, I.J. Fuss, N. Bouladoux, M.H. Askenase, F. Legrand, L.Y. Koo, J.M. Brenchley, I.D.C. Fraser, and Y. Belkaid. 2013. Inflammatory monocytes regulate pathologic responses to commensals during acute gastrointestinal infection. *Nat. Med.* 19:713–721. http://dx.doi.org/10.1038/nm.3189

Haeberle, H.A., W.A. Kuziel, H.J. Dieterich, A. Casola, Z. Gatalica, and R.P. Garofalo. 2001. Inducible expression of inflammatory chemokines in respiratory syncytial virus-infected mice: role of MIP-1α in lung pathology. *J. Virol.* 75:878–890. http://dx.doi.org/10.1128/JVI.75.2.878-890.2001

Helft, J., B. Manicassamy, P. Guermonprez, D. Hashimoto, A. Silvin, J. Agudo, B.D. Brown, M. Schmolke, J.C. Miller, M. Leboeuf, et al. 2012. Cross-presenting CD103$^+$ dendritic cells are protected from influenza virus infection. *J. Clin. Invest.* 122:4037–4047. http://dx.doi.org/10.1172/JCI60659

Herold, S., M. Steinmueller, W. von Wulffen, L. Cakarova, R. Pinto, S. Pleschka, M. Mack, W.A. Kuziel, N. Corazza, T. Brunner, et al. 2008. Lung epithelial apoptosis in influenza virus pneumonia: the role of macrophage-expressed TNF-related apoptosis-inducing ligand. *J. Exp. Med.* 205:3065–3077. http://dx.doi.org/10.1084/jem.20080201

Hussell, T., and T.J. Bell. 2014. Alveolar macrophages: plasticity in a tissue-specific context. *Nat. Rev. Immunol.* 14:81–93. http://dx.doi.org/10.1038/nri3600

Iijima, N., L.M. Mattei, and A. Iwasaki. 2011. Recruited inflammatory monocytes stimulate antiviral Th1 immunity in infected tissue. *Proc. Natl. Acad. Sci. USA.* 108:284–289. http://dx.doi.org/10.1073/pnas.1005201108

Janssen, R., L. Bont, C.L.E. Siezen, H.M. Hodemaekers, M.J. Ermers, G. Doornbos, R. van 't Slot, C. Wijmenga, J.J. Goeman, J.L. Kimpen, et al. 2007. Genetic susceptibility to respiratory syncytial virus bronchiolitis is predominantly associated with innate immune genes. *J. Infect. Dis.* 196:826–834. http://dx.doi.org/10.1086/520886

Jewell, N.A., N. Vaghefi, S.E. Mertz, P. Akter, R.S. Peebles Jr., L.O. Bakaletz, R.K. Durbin, E. Flaño, and J.E. Durbin. 2007. Differential type I interferon induction by respiratory syncytial virus and influenza a virus in vivo. *J. Virol.* 81:9790–9800. http://dx.doi.org/10.1128/JVI.00530-07

Kumagai, Y., O. Takeuchi, H. Kato, H. Kumar, K. Matsui, E. Morii, K. Aozasa, T. Kawai, and S. Akira. 2007. Alveolar macrophages are the primary interferon-alpha producer in pulmonary infection with RNA viruses. *Immunity*. 27:240–252. http://dx.doi.org/10.1016/j.immuni.2007.07.013

Lee, D.C.P., J.A.E. Harker, J.S. Tregoning, S.F. Atabani, C. Johansson, J. Schwarze, and P.J.M. Openshaw. 2010. CD25$^+$ natural regulatory T cells are critical in limiting innate and adaptive immunity and resolving disease following respiratory syncytial virus infection. *J. Virol.* 84:8790–8798. http://dx.doi.org/10.1128/JVI.00796-10

Lin, K.L., Y. Suzuki, H. Nakano, E. Ramsburg, and M.D. Gunn. 2008. CCR2$^+$ monocyte-derived dendritic cells and exudate macrophages produce influenza-induced pulmonary immune pathology and mortality. *J. Immunol.* 180:2562–2572. http://dx.doi.org/10.4049/jimmunol.180.4.2562

Ling, Z., K.C. Tran, and M.N. Teng. 2009. Human respiratory syncytial virus nonstructural protein NS2 antagonizes the activation of beta interferon transcription by interacting with RIG-I. *J. Virol.* 83:3734–3742. http://dx.doi.org/10.1128/JVI.02434-08

Liu, P., M. Jamaluddin, K. Li, R.P. Garofalo, A. Casola, and A.R. Brasier. 2007. Retinoic acid-inducible gene I mediates early antiviral response and Toll-like receptor 3 expression in respiratory syncytial virus-infected airway epithelial cells. *J. Virol.* 81:1401–1411. http://dx.doi.org/10.1128/JVI.01740-06

Loebbermann, J., H. Thornton, L. Durant, T. Sparwasser, K.E. Webster, J. Sprent, F.J. Culley, C. Johansson, and P.J. Openshaw. 2012. Regulatory T cells expressing granzyme B play a critical role in controlling lung inflammation during acute viral infection. *Mucosal Immunol.* 5:161–172. http://dx.doi.org/10.1038/mi.2011.62

Loo, Y.-M., J. Fornek, N. Crochet, G. Bajwa, O. Perwitasari, L. Martinez-Sobrido, S. Akira, M.A. Gill, A. García-Sastre, M.G. Katze, and M. Gale Jr. 2008. Distinct RIG-I and MDA5 signaling by RNA viruses in innate immunity. *J. Virol.* 82:335–345. http://dx.doi.org/10.1128/JVI.01080-07

Mack, M., J. Cihak, C. Simonis, B. Luckow, A.E. Proudfoot, J. Plachý, H. Brühl, M. Frink, H.J. Anders, V. Vielhauer, et al. 2001. Expression and characterization of the chemokine receptors CCR2 and CCR5 in mice. *J. Immunol.* 166:4697–4704. http://dx.doi.org/10.4049/jimmunol.166.7.4697

Majer, O., C. Bourgeois, F. Zwolanek, C. Lassnig, D. Kerjaschki, M. Mack, M. Müller, and K. Kuchler. 2012. Type I interferons promote fatal immunopathology by regulating inflammatory monocytes and neutrophils during Candida infections. *PLoS Pathog.* 8:e1002811. http://dx.doi.org/10.1371/journal.ppat.1002811

Marr, N., S.E. Turvey, and N. Grandvaux. 2013. Pathogen recognition receptor crosstalk in respiratory syncytial virus sensing: a host and cell type perspective. *Trends Microbiol.* 21:568–574. http://dx.doi.org/10.1016/j.tim.2013.08.006

McNamara, P.S., B.F. Flanagan, C.A. Hart, and R.L. Smyth. 2005. Production of chemokines in the lungs of infants with severe respiratory syncytial virus bronchiolitis. *J. Infect. Dis.* 191:1225–1232. http://dx.doi.org/10.1086/428855

Merolla, R., N.A. Rebert, P.T. Tsiviste, S.P. Hoffmann, and J.R. Panuska. 1995. Respiratory syncytial virus replication in human lung epithelial cells: inhibition by tumor necrosis factor alpha and interferon beta. *Am. J. Respir. Crit. Care Med.* 152:1358–1366. http://dx.doi.org/10.1164/ajrccm.152.4.7551395

Messier, E.M., R.J. Mason, and B. Kosmider. 2012. Efficient and rapid isolation and purification of mouse alveolar type II epithelial cells. *Exp. Lung Res.* 38:363–373. http://dx.doi.org/10.3109/01902148.2012.713077

Miller, A.L., T.L. Bowlin, and N.W. Lukacs. 2004. Respiratory syncytial virus-induced chemokine production: linking viral replication to chemokine production in vitro and in vivo. *J. Infect. Dis.* 189:1419–1430. http://dx.doi.org/10.1086/382958

Narasaraju, T., H.H. Ng, M.C. Phoon, and V.T.K. Chow. 2010. MCP-1 antibody treatment enhances damage and impedes repair of the alveolar epithelium in influenza pneumonitis. *Am. J. Respir. Cell Mol. Biol.* 42:732–743. http://dx.doi.org/10.1165/rcmb.2008-0423OC

Perkins, S.M., D.L. Webb, S.A. Torrance, C. El Saleeby, L.M. Harrison, J.A. Aitken, A. Patel, and J.P. DeVincenzo. 2005. Comparison of a real-time reverse transcriptase PCR assay and a culture technique for quantitative assessment of viral load in children naturally infected with respiratory syncytial virus. *J. Clin. Microbiol.* 43:2356–2362. http://dx.doi.org/10.1128/JCM.43.5.2356-2362.2005

Plantinga, M., M. Guilliams, M. Vanheerswynghels, K. Deswarte, F. Branco-Madeira, W. Toussaint, L. Vanhoutte, K. Neyt, N. Killeen, B. Malissen, et al. 2013. Conventional and monocyte-derived CD11b$^+$ dendritic cells initiate and maintain T helper 2 cell-mediated immunity to house dust mite allergen. *Immunity*. 38:322–335. http://dx.doi.org/10.1016/j.immuni.2012.10.016

Pribul, P.K., J. Harker, B. Wang, H. Wang, J.S. Tregoning, J. Schwarze, and P.J.M. Openshaw. 2008. Alveolar macrophages are a major determinant of early responses to viral lung infection but do not influence subsequent disease development. *J. Virol.* 82:4441–4448. http://dx.doi.org/10.1128/JVI.02541-07

Ravi, L.I., L. Li, R. Sutejo, H. Chen, P.S. Wong, B.H. Tan, and R.J. Sugrue. 2013. A systems-based approach to analyse the host response in murine lung macrophages challenged with respiratory syncytial virus. *BMC Genomics*. 14:190. http://dx.doi.org/10.1186/1471-2164-14-190

Rutigliano, J.A., and B.S. Graham. 2004. Prolonged production of TNF-α exacerbates illness during respiratory syncytial virus infection. *J. Immunol.* 173:3408–3417. http://dx.doi.org/10.4049/jimmunol.173.5.3408

Samstein, M., H.A. Schreiber, I.M. Leiner, B. Susac, M.S. Glickman, and E.G. Pamer. 2013. Essential yet limited role for CCR2$^+$ inflammatory monocytes during *Mycobacterium tuberculosis*-specific T cell priming. *eLife*. 2:e01086.

Scagnolari, C., F. Midulla, C. Selvaggi, K. Monteleone, E. Bonci, P. Papoff, G. Cangiano, P. Di Marco, C. Moretti, A. Pierangeli, and G. Antonelli. 2012. Evaluation of viral load in infants hospitalized with bronchiolitis caused by respiratory syncytial virus. *Med. Microbiol. Immunol. (Berl.).* 201:311–317. http://dx.doi.org/10.1007/s00430-012-0233-6

Schijf, M.A., M.V. Lukens, D. Kruijsen, N.O.P. van Uden, J. Garssen, F.E.J. Coenjaerts, B. Van't Land, and G.M. van Bleek. 2013. Respiratory syncytial virus induced type I IFN production by pDC is regulated by RSV-infected airway epithelial cells, RSV-exposed monocytes and virus

specific antibodies. *PLoS ONE*. 8:e81695. http://dx.doi.org/10.1371/journal.pone.0081695

Schoggins, J.W., D.A. MacDuff, N. Imanaka, M.D. Gainey, B. Shrestha, J.L. Eitson, K.B. Mar, R.B. Richardson, A.V. Ratushny, V. Litvak, et al. 2014. Pan-viral specificity of IFN-induced genes reveals new roles for cGAS in innate immunity. *Nature*. 505:691–695. http://dx.doi.org/10.1038/nature12862

Segura, E., M. Touzot, A. Bohineust, A. Cappuccio, G. Chiocchia, A. Hosmalin, M. Dalod, V. Soumelis, and S. Amigorena. 2013. Human inflammatory dendritic cells induce Th17 cell differentiation. *Immunity*. 38:336–348. http://dx.doi.org/10.1016/j.immuni.2012.10.018

Seo, S.-U., H.-J. Kwon, H.-J. Ko, Y.-H. Byun, B.L. Seong, S. Uematsu, S. Akira, and M.-N. Kweon. 2011. Type I interferon signaling regulates Ly6C^{hi} monocytes and neutrophils during acute viral pneumonia in mice. *PLoS Pathog*. 7:e1001304. http://dx.doi.org/10.1371/journal.ppat.1001304

Serbina, N.V., and E.G. Pamer. 2006. Monocyte emigration from bone marrow during bacterial infection requires signals mediated by chemokine receptor CCR2. *Nat. Immunol*. 7:311–317. http://dx.doi.org/10.1038/ni1309

Serbina, N.V., T.P. Salazar-Mather, C.A. Biron, W.A. Kuziel, and E.G. Pamer. 2003. TNF/iNOS-producing dendritic cells mediate innate immune defense against bacterial infection. *Immunity*. 19:59–70. http://dx.doi.org/10.1016/S1074-7613(03)00171-7

Shi, C., and E.G. Pamer. 2011. Monocyte recruitment during infection and inflammation. *Nat. Rev. Immunol*. 11:762–774. http://dx.doi.org/10.1038/nri3070

Siezen, C.L.E., L. Bont, H.M. Hodemaekers, M.J. Ermers, G. Doornbos, R. Van't Slot, C. Wijmenga, H.C. Houwelingen, J.L.L. Kimpen, T.G. Kimman, et al. 2009. Genetic susceptibility to respiratory syncytial virus bronchiolitis in preterm children is associated with airway remodeling genes and innate immune genes. *Pediatr. Infect. Dis. J*. 28:333–335. http://dx.doi.org/10.1097/INF.0b013e31818e2aa9

Slater, L., N.W. Bartlett, J.J. Haas, J. Zhu, S.D. Message, R.P. Walton, A. Sykes, S. Dahdaleh, D.L. Clarke, M.G. Belvisi, et al. 2010. Co-ordinated role of TLR3, RIG-I and MDA5 in the innate response to rhinovirus in bronchial epithelium. *PLoS Pathog*. 6:e1001178. http://dx.doi.org/10.1371/journal.ppat.1001178

Smit, J.J., B.D. Rudd, and N.W. Lukacs. 2006. Plasmacytoid dendritic cells inhibit pulmonary immunopathology and promote clearance of respiratory syncytial virus. *J. Exp. Med*. 203:1153–1159. http://dx.doi.org/10.1084/jem.20052359

Spann, K.M., K.C. Tran, B. Chi, R.L. Rabin, and P.L. Collins. 2004. Suppression of the induction of alpha, beta, and lambda interferons by the NS1 and NS2 proteins of human respiratory syncytial virus in human epithelial cells and macrophages [corrected]. *J. Virol*. 78:4363–4369. http://dx.doi.org/10.1128/JVI.78.8.4363-4369.2004

Stark, J.M., A.M. Khan, C.L. Chiappetta, H. Xue, J.L. Alcorn, and G.N. Colasurdo. 2005. Immune and functional role of nitric oxide in a mouse model of respiratory syncytial virus infection. *J. Infect. Dis*. 191:387–395. http://dx.doi.org/10.1086/427241

Tal, G., A. Mandelberg, I. Dalal, K. Cesar, E. Somekh, A. Tal, A. Oron, S. Itskovich, A. Ballin, S. Houri, et al. 2004. Association between common Toll-like receptor 4 mutations and severe respiratory syncytial virus disease. *J. Infect. Dis*. 189:2057–2063. http://dx.doi.org/10.1086/420830

Tulic, M.K., R.J. Hurrelbrink, C.M. Prêle, I.A. Laing, J.W. Upham, P. Le Souef, P.D. Sly, and P.G. Holt. 2007. TLR4 polymorphisms mediate impaired responses to respiratory syncytial virus and lipopolysaccharide. *J. Immunol*. 179:132–140. http://dx.doi.org/10.4049/jimmunol.179.1.132

Welliver, R.C., R.P. Garofalo, and P.L. Ogra. 2002. Beta-chemokines, but neither T helper type 1 nor T helper type 2 cytokines, correlate with severity of illness during respiratory syncytial virus infection. *Pediatr. Infect. Dis. J*. 21:457–461. http://dx.doi.org/10.1097/00006454-200205000-00033

Yoboua, F., A. Martel, A. Duval, E. Mukawera, and N. Grandvaux. 2010. Respiratory syncytial virus-mediated NF-κB p65 phosphorylation at serine 536 is dependent on RIG-I, TRAF6, and IKKβ. *J. Virol*. 84:7267–7277. http://dx.doi.org/10.1128/JVI.00142-10